AD-A040 347 OHIO STATE UNIV COLUMBUS ELECTROSCIENCE LAB F/G 17/9
CONTINUATION OF THE INVESTIGATION OF THE MULTI-FREQUENCY RADAR --ETC(U)
MAR 77 C D CHUANG, D L MOFFATT, L PETERS F19628-72-C-0203
UNCLASSIFIED ESL-3424-7 RADC-TR-77-115 NL

| OF |
AD
A040347

END

DATE
FILMED
7-77

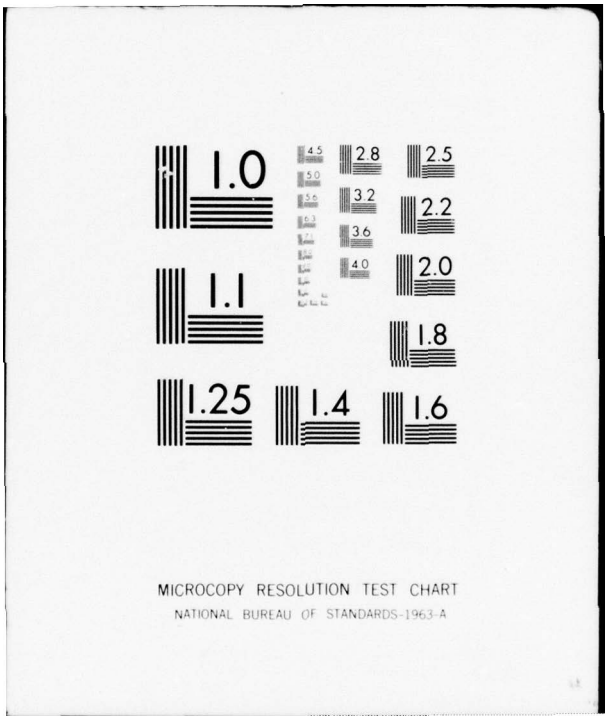
1.0
1.1
1.25
1.4
1.6
1.8
2.0
2.2
2.5
2.8
3.2
3.6
4.0
4.5
5.0
5.6
MICROCOPY RESOLUTION TEST CHART
NATIONAL BUREAU OF STANDARDS-1963-A

AD A040347

RADC-TR-77-115
Final Technical Report
March 1977

CONTINUATION OF THE INVESTIGATION OF THE MULTI-FREQUENCY RADAR REFLECTIVITY OF RADAR TARGET IDENTIFICATION

The Ohio State University ElectroScience Laboratory

Approved for public release; distribution unlimited.

DDC
RECEIVED
JUN 9 1977
D

ROME AIR DEVELOPMENT CENTER
AIR FORCE SYSTEMS COMMAND
GRIFFISS AIR FORCE BASE, NEW YORK 13441

AD No.
DDC FILE COPY

Professor David L. Moffatt is the responsible investigator for the radar target identification investigation and Professor Leon Peters, Jr., is the responsible investigator for the radar cross section control investigation under this contract. Dr. Richard B. Mack (ETER) is the RADC Project Engineer.

This report has been reviewed by the RADC Information Office (OI) and is releasable to the National Technical Information Service (NTIS). At NTIS it will be releasable to the General public, including foreign nations.

This technical report has been reviewed and approved for publication.

APPROVED:

Richard B. Mack
RICHARD B. MACK
Project Engineer

APPROVED: Allan C. Schell
ALLAN C. SCHELL
Acting Chief
Electromagnetic Sciences Division

FOR THE COMMANDER: John P. Huss

Plans Office

UNCLASSIFIED

SECURITY CLASSIFICATION OF THIS PAGE *(When Data Entered)*

REPORT DOCUMENTATION PAGE

READ INSTRUCTIONS BEFORE COMPLETING FORM

1. REPORT NUMBER: RADC-TR-77-115	2. GOVT ACCESSION NO.
3. RECIPIENT'S CATALOG NUMBER	
4. TITLE *(and Subtitle)*: CONTINUATION OF THE INVESTIGATION OF THE MULTI-FREQUENCY RADAR REFLECTIVITY OF RADAR TARGET IDENTIFICATION	5. TYPE OF REPORT & PERIOD COVERED: Final 4/10/72-9/30/76
	6. PERFORMING ORG. REPORT NUMBER: ESL-3424-7
7. AUTHOR(s): C.D. Chuang, D.L. Moffatt, E. Peters, Jr., K.A. Shubert	8. CONTRACT OR GRANT NUMBER(s): F19628-72-C-0203
9. PERFORMING ORGANIZATION NAME AND ADDRESS: The Ohio State University ElectroScience Laboratory, Department of Electrical Engineering Columbus, Ohio 43212	10. PROGRAM ELEMENT, PROJECT, TASK AREA & WORK UNIT NUMBERS: 61102F 56350204 02
11. CONTROLLING OFFICE NAME AND ADDRESS: Deputy for Electronic Technology (RADC) Hanscom AFB, Massachusetts 01731 Monitor/Richard Mack/ETER	12. REPORT DATE: March 1977
	13. NUMBER OF PAGES: 58
14. MONITORING AGENCY NAME & ADDRESS *(if different from Controlling Office)*	15. SECURITY CLASS. *(of this report)*: Unclassified
	15a. DECLASSIFICATION/DOWNGRADING SCHEDULE

16. DISTRIBUTION STATEMENT *(of this Report)*

Approved for public release;
distribution unlimited

17. DISTRIBUTION STATEMENT *(of the abstract entered in Block 20, if different from Report)*

18. SUPPLEMENTARY NOTES

402 251

19. KEY WORDS *(Continue on reverse side if necessary and identify by block number)*

Target identification	Nonspecular
Aircraft	Scattering
Transients	Loading
Radar	Control

20. ABSTRACT *(Continue on reverse side if necessary and identify by block number)*

Research on Contract No. F19628-72-C-0203 during the period 10 April 1972 to 30 September 1976 is summarized. Two subjects of significance to the Air Force, radar target identification and control of nonspecular scattering, have been studied. Progress in each area has been described in a series of Scientific Reports. These results are briefly summarized. More recent efforts, not yet completed, are discussed in more detail. Conclusions and recommendations for future research and implementation are made.

DD FORM 1 JAN 73 1473 EDITION OF 1 NOV 65 IS OBSOLETE

UNCLASSIFIED

SECURITY CLASSIFICATION OF THIS PAGE *(When Data Entered)*

EVALUATION

1. This report is the Final Report on Contract F19628-72-C-0203. It summarizes the research done during the period from April 1972 through September 1976. The objectives of the research were to investigate multiple-frequency method of target identifications based on pole-zero representations of the natural electromagnetic resonances of the radar targets and to investigate the possibilities of controlling nonspecular radar cross sections of extended reflectors by impedance loading methods. The results that are summarized in the report have shown that aircraft recognition is possible using as few as three harmonically related frequencies, and that the lowest resonances are aspect invariant. They also show that a control range of over 20dB can be obtained over significant angular intervals in the leading and trailing edge directions of wing-like structures. This work was part of a research effort aimed at developing new alternative methods of radar target identification.

2. The above work is of value because it provides basic knowledge and concepts on which different and advantageous methods of radar target identification can be based.

Richard B. Mack

RICHARD B. MACK
Project Engineer

ACCESSION for
NTIS White Section ☒
DDC Buff Section ☐
UNANNOUNCED ☐
JUSTIFICATION
BY
DISTRIBUTION/AVAILABILITY CODES
Dist. AVAIL. and/or SPECIAL
A

DDC
RECEIVED
JUN 9 1977
D

PRECEDING PAGE BLANK-NOT FILMED

PERSONNEL

During this contract period the following personnel have contributed to the research effort.

John Aas
John Apinis
C. F. Chuang
Edward M. Kennaugh
S. C. Lee
R. K. Mains
David L. Moffatt
Leon Peters
Jack H. Richmond
Roger Rudduck
Keith Shubert

PRECEDING PAGE BLANK-NOT FILMED

REPORTS, PAPERS, AND ORAL PRESENTATIONS ON CONTRACT F19628-72-C-0203

Reports

3424-1, "Complex Natural Resonances of an Object in Detection and Discrimination, R. K. Mains and D. L. Moffatt, June 1974.

3424-2, "Control of Electromagnetic Scattering by Antenna Impedance Loading," S. C. Lee, July 1974.

3424-3, "Complex Natural Resonances of Radar Targets Via Prony's Method," C. D. Chuang and D. L. Moffatt.

3424-4, "Control of Electromagnetic Scattering from Wing Profiles by Impedance Loading," J. Aas, August 1975.

3424-5, "Continuation of the Investigation of Multi-Frequency Radar Reflectivity and Radar Target Identification," D. L. Moffatt, R. C. Rudduck, C. D. Chuang, J. A. Aas, July 1975.

3424-6, "Reduction of Backscattering by Impedance Loading," C. W. Chuang, October 1976.

3424-7, Final Report on Continuation of the Investigation of the Multi-Frequency Radar Reflectivity of Radar Target Identification, C. D. Chuang, D. L. Moffatt, L. Peters, Jr., K. A. Shubert, December 1976.

Papers

David L. Moffatt and Keith A. Shubert, "Natural Resonances Via Rational Function Approximations," submitted for publication to IEEE Trans. on Antennas and Propagation, July, 1976.

C. D. Chuang and David L. Moffatt, "Natural Resonances of Radar Targets Via Prony's Method and Target Discrimination," IEEE Trans. on Aerospace and Electronic Systems, Vol. 12, No. 5, September, 1976.

E. M. Kennaugh and D. L. Moffatt, "Impulse and Transient Response Approximations," 1976 Short Course Notes on Radar Target Identification, Ohio State University, September 10-12, 1976.

David L. Moffatt, "Radar Target Detection and Discrimination," 1976 Short Course Notes on Radar Target Identification, Ohio State University, September 10-12, 1976.

PRECEDING PAGE BLANK-NOT FILMED

C. D. Chuang and David L. Moffatt, "Noise Effects in Predictor Correlator Processing," 1976 Short Course Notes on Radar Target Identification, Ohio State University, September 10-12, 1976.

David L. Moffatt and Richard K. Mains, "Radar Target Detection and Discrimination," IEEE Trans. on Antennas and Propagation, Vol. AP-23, No. 3, May 1975.

David L. Moffatt, Robert H. Paul and Robert A. Voss, Correction to "The Echo Area of a Perfectly Conducting Prolate Spheroid," IEEE Trans. on Antennas and Propagation, March, 1973.

Oral Presentations

David L. Moffatt, "A New Approach to the Identification of Space Objects," 1976 NORAD Meeting, Norsic 8 on Spacecraft Identification, Colorado Springs, Colorado, August 2-6, 1976.

C. D. Chuang and D. L. Moffatt, "Noise Effects in Predictor-Corralator Processing," 1976 URSI Meeting, Boulder, Colorado, June, 1976.

David L. Moffatt, "Complex Natural Resonances of Radar Targets in Detection and Discrimination," Review Meeting on Natural Resonances held at RADC, Rome, N.Y., November 16, 1975.

C. D. Chuang and D. L. Moffatt, "Complex Natural Resonances of Radar Targets Via Prony's Method," 1975 URSI Meeting, University of Illinois, Urbana, Illinois, June 3-5, 1975.

D. L. Moffatt, J. H. Richmond and R. K. Mains, "Complex Natural Resonances of an Object in Detection and Discrimination," G-AP International Symposium, University of Colorado, Boulder, Colorado, August, 1973.

CONTENTS

I. INTRODUCTION

Very significant progress on two problems of major interest to the Air Force, identification of radar targets and control of nonspecular scattering, has been achieved during this contract period. This report summarizes these results, citing reports and publications where appropriate and giving more detailed discussions of latest as yet unpublished results.

The radar target identification problem has been approached from a fundamental point of view. That is, the impulse response concept was used to define that response waveform, the ramp response waveform, most intimately associated with the gross physical (size, shape, and composition) properties of the target. This also dictated the proper spectral range for the interrogating radar signal. It was recognized that for times after the interrogating signal moved beyond the object, the waveforms were amenable to approximation by finite exponential sums. This established the dominant complex natural resonances of the target as an excitation invariant set of target descriptors. Using the natural resonances, target discrimination was conclusively demonstrated for both simple shapes and realistic models of the F-4, F-104 and MIG-19 aircraft.

It should be noted that the approach to the target identification problem described above is in direct contrast to an approach which starts with data obtainable by presently operational radars. This latter approach has been notably unsuccessful for the identification problem. Assuming that the dominant resonances of an object can be obtained, and this appears to be reasonably well in hand, two general problems can be identified in considering implementation of our discrimination scheme. Discrete multiple frequency scattering data are needed and the required frequencies are relatively low. Most recent efforts have been directed toward methods for reducing the complexity of the required radar data. As detailed herein some progress in this direction has been made. In addition, a suggestion for drastically raising the interrogating radar spectrum is outlined in the recommendations section. The effect of noise on the discrimination process has been studied using a very simple model. On the basis of these results changes in the discrimination process to reduce the effects of noise have been made. The changes also yield a more easily interpretable discrimination test.

PRECEDING PAGE BLANK-NOT FILMED

The suppression of scattering is a camouflage problem, but over the years the development of techniques for the reduction of specular contributions has received most attention. Although the specular contributions tend to be restricted in the aspect angles for which they occur, they dominate the net return whenever they are present. However, the specular echoes are amenable to suppression using radar absorbents. On the other hand, nonspecular scattering is more pervasive. Even if all specular echoes are suppressed, the non-specular scattering still can generate radar returns of unacceptable magnitude. In fact, modern aerospace vehicles are seldom seen at specular aspects in a tactical environment. But the nonspecular radar cross section can still reach levels that increases the probability of detection. It is therefore important to study the backscatter reduction in non-specular aspects.

The earlier studies have involved the study of scattering from the trailing edge of square flat plates and 2-D wing foil geometries [11]. The square flat plate involved the use of a loaded slot to control the back scattered fields from the trailing edge for polarization perpendicular to the edge. At this time, it would appear that this result could be improved if a longer slot had been used so that its length is comparable to that of the edge whose radar cross section is to be reduced. The 2-D wing foil was analyzed using strips of surface impedance for echo area control. To obtain accurate results, a novel form of a hybrid moment method solution was introduced involving an additional term of the form

$$\frac{C_1 e^{-jkr}}{\sqrt{r}}$$

where r is the distance from the edge and C_1 is an unknown constant. The study of diffraction, from the leading edge, the dominant component for parallel polarization required an additional term proportional to $(r)^{-3/2}$ power be included [12]. Further, for grazing incidence on the strip an unknown constant term was needed [6].

Finally a folded dipole geometry was introduced [13,14]. This geometry included two impedance loads, one at the terminals and another at the end which when transformed to terminals would represent an open circuit in so far as the transmission line mode is concerned. The research in the last year focussed on optimizing the RCS reduction achieved with this type of impedance loading. The results were certainly encouraging.

II. TARGET IDENTIFICATION

At the beginning of this contract it was known that the dominant natural resonances of a radar target, modeled as simple poles, formed an excitation invariant set of target descriptors. That is, the poles are independent of the target orientation or radar polarization. It was also known that a synthetically produced ramp response waveform, intimately related to the gross physical properties of the target, was one appropriate identification signal. An identification scheme, predictor-correlator processing, had been successfully tested using the known poles of conducting spheres and slender prolate spheroids [1].

A number of problems remained to be addressed. The most serious of these was the lack of a good procedure of locating the dominant poles of an arbitrary structure. Rational function fits of real multiple frequency scattering data had shown promise but were not precise [2]. A second problem which had not been studied was the effects of noise on the identification process. Thirdly only simple classical shapes had been identified, the extension to realistic target geometries remained. As summarized below, substantial progress has been achieved in all of these problem areas.

Three methods for obtaining the complex natural resonances of radar targets have now been successfully tested. The first method applies an iterative search procedure to an integral equation formulation of the target as a radiator. As examples, the dominant natural resonances of simple models of straight and swept wing aircraft are shown as open circles in Figures 1 and 2 respectively. The crosses are by another method to be discussed. These results are given in [3,4] as are the poles of bent and configurations of perpendicularly crossed wires. The iterative search procedure has the advantage that it always correctly identifies the dominant poles of the structure. However, the method requires that a wire grid model of the scatterer be formulated via an integral equation. For complex structures such as aircraft [5], where many wire segments are required, the iterative search procedure becomes prohibitively lengthy. In addition the search procedure is somewhat cumbersome if good first estimates of all the dominant poles cannot be made.

Backscatter calculations (amplitude and phase) for $L/\lambda=0.05(0.05)0.5$ were made on both the straight and swept wing models for (Figure 1) $\hat{\phi}$ polarization in the $\theta=\pi/2$ plane for $\phi=-90°(15°)90°$ and $\hat{\theta}$ polarization in the $\phi=\pi/2$ plane for $\theta=0°(15°)180°$. Discrimination tests using these data are completely reported in [3] and representative results given in [4]. The discrimination test, unity minus the normalized squared error between a measured and calculated waveform, is described completely in [3] and [4]. Successful discrimination was achieved at all aspects and polarizations except near nose-on and tail-on. Failure in these regions was due to the lack of excitation of the wing and horizontal stabilizers, i.e., higher frequency data were needed. Examples are shown in Figures 3 and 4. Note that threshold levels could be set in each case.

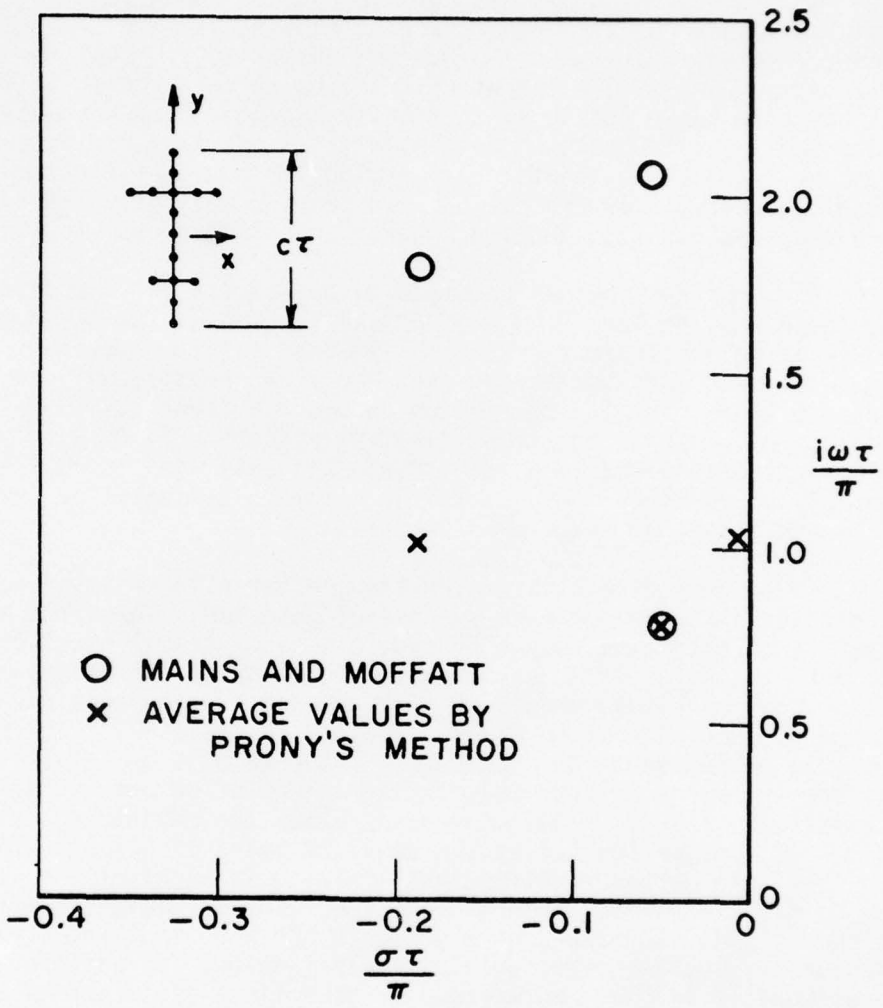

Figure 1. Natural resonances of a straight wing aircraft model.

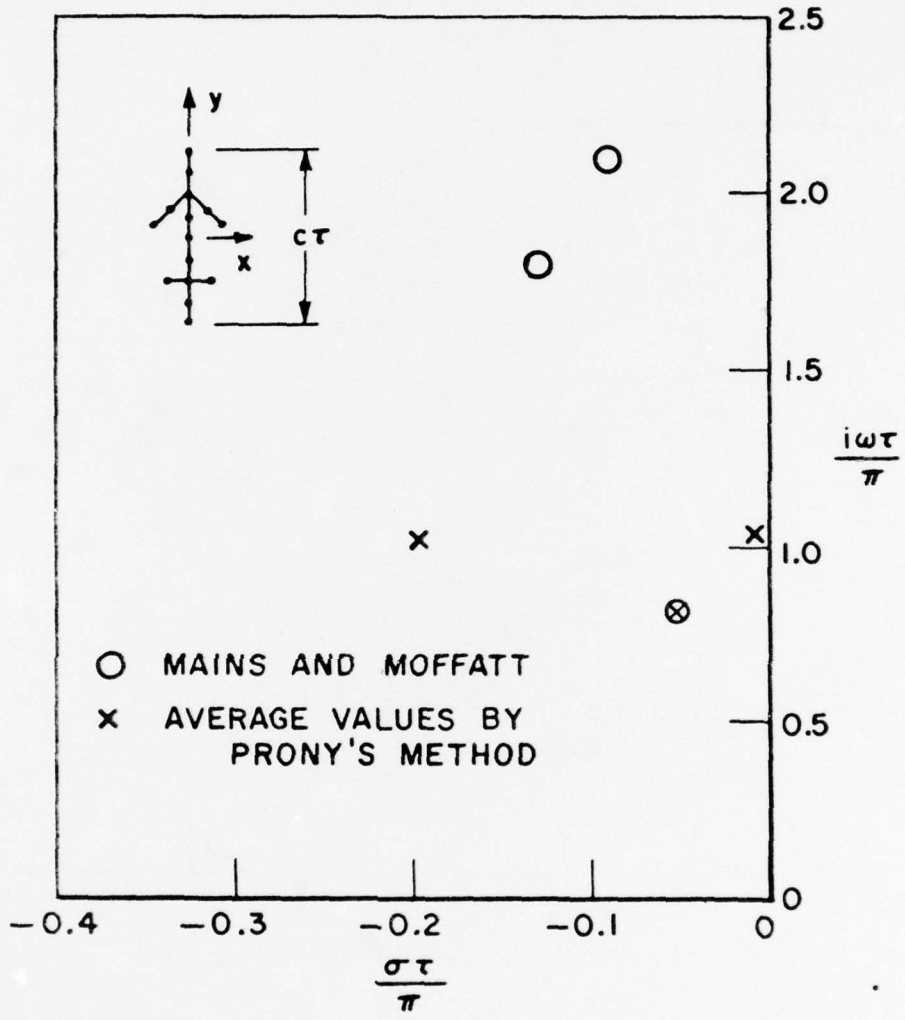

Figure 2. Natural resonances of a swept wing aircraft model.

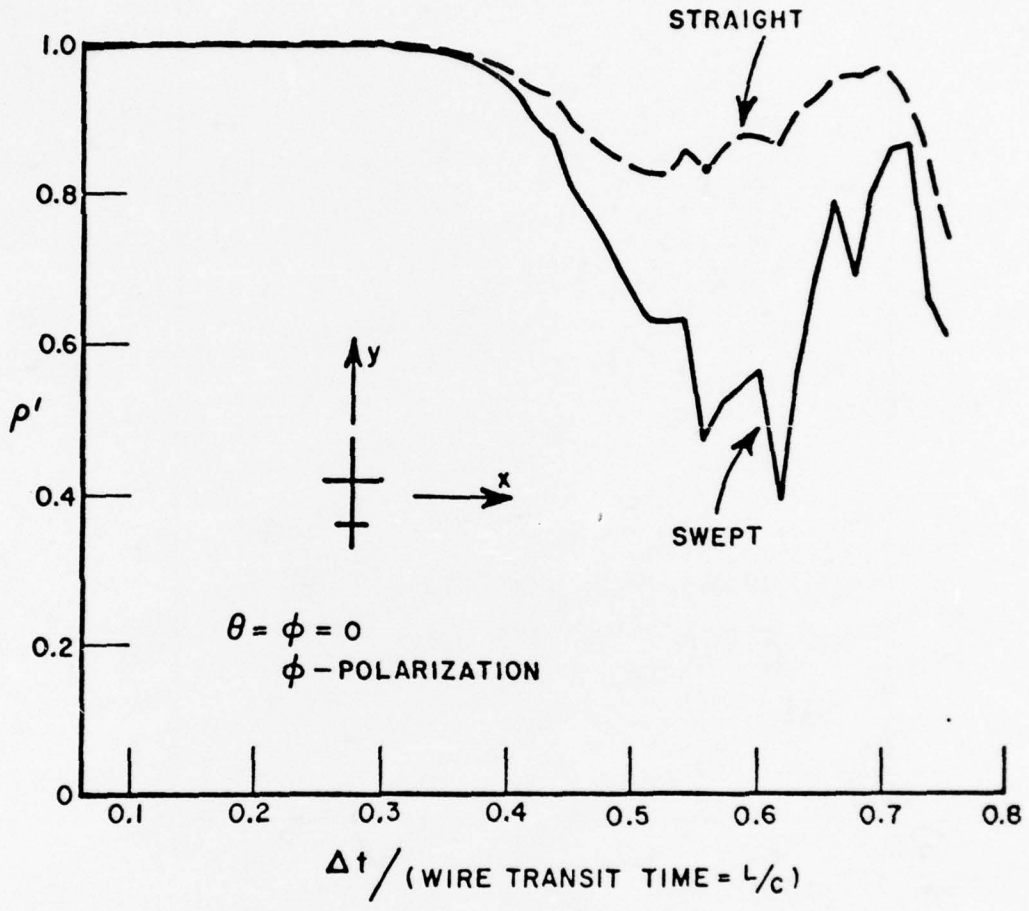

Figure 3. Calculation of ρ' for the structures of Figures 1 and 2, using natural resonances of the straight wing model.

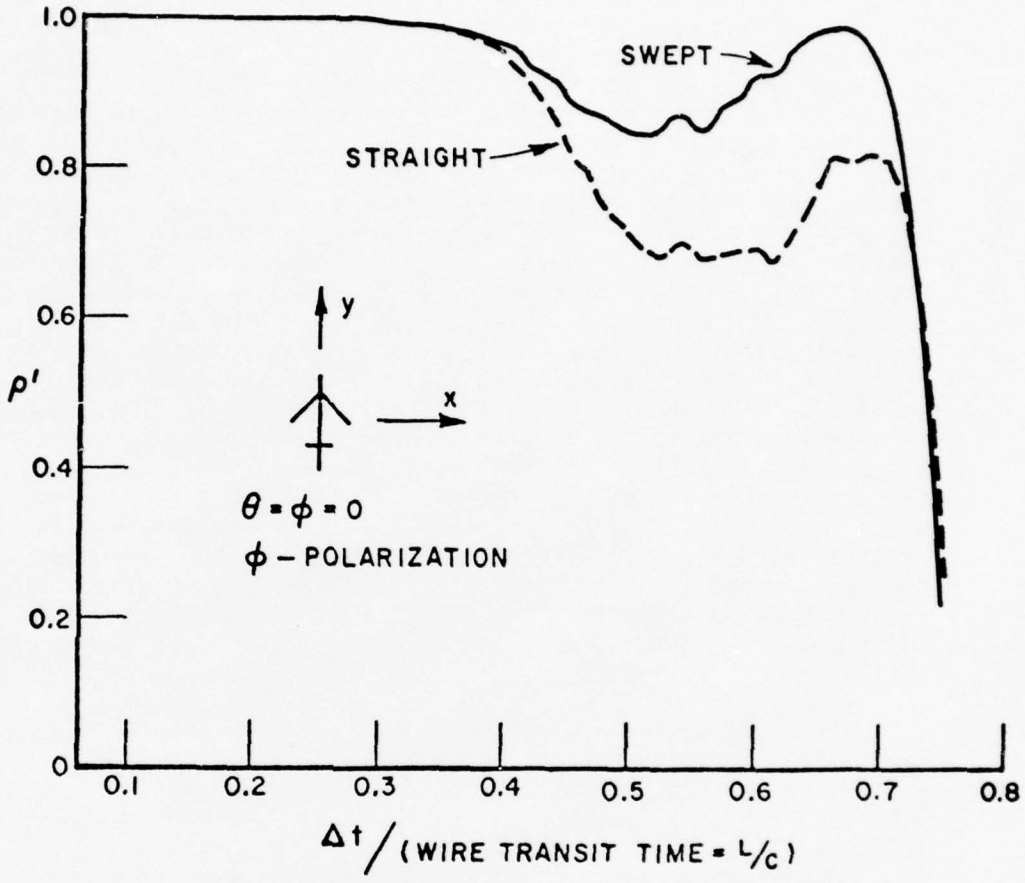

Figure 4. Calculation of ρ' for the structures of Figures 1 and 2, using natural resonances of the swept wing model.

A second method of determining dominant natural resonances of a structure is via Prony's method. Prony's method is an algorithm for fitting a finite sum of exponentials to a transient response waveform. Thus the method is applicable in principle to transient response waveforms obtained experimentally or numerically. The poles of the straight and swept wing aircraft as obtained from synthesized ramp response waveforms are shown as crosses in Figures 1 and 2. Note that agreement is obtained for only one pole. The reason for this is that the higher poles as obtained by numerical search are not excited by the scattering data used to synthesize the ramp response waveforms. This points out one weakness of the Prony method. The number of poles to be extracted must be specified in advance. In addition to the simple aircraft, Prony's method has also been applied to conducting spheres, prolate spheroids, and realistic models of the F-4, F-104 and MIG-19 aircraft [5]. These pole results are completely reported in [6] and representative results given in [7]. The poles of the F-4, F-104 and MIG-19 aircraft are given in Tables 1, 2 and 3. These tables illustrate a problem which arises with the Prony method. For the orientation data given in the tables, the aircraft fuselage is along the z axis with the nose in the plus z direction and the wings are along the y axis. For changes in the aircraft orientation the poles obtained do not remain precisely invariant. Those marked as (d) had dominant residues. This means that averages must be used. Similar results have been obtained (on a related Grant AFOSR 69-1710A) on five additional aircraft. Thus while the Prony method can be used to obtain pole locations, a certain amount of trial and error is involved.

Using the poles obtained by Prony's method, discrimination tests were made on both the simple and realistic aircraft models. Successful discrimination was achieved for both types of targets. These are reported completely in [6] and the realistic aircraft results are given in [7]. It is noted that for the stick models better discrimination was achieved using the Prony poles and, in fact, failure in the nose-on and tail-on regions disappeared. Examples of discrimination for the realistic aircraft models are shown in Figures 5, 6 and 7.

A comparison of results on the simple aircraft models using the Prony and iterative search poles shows that for the iterative search poles, discrimination was based almost entirely on one pole location (and its complex conjugate), that with lowest oscillatory frequency in Figures 1 and 2. This further explains why it was possible to delete amplitude and phase scattering data at the four lowest harmonics and phase data at the fifth, sixth and seventh harmonics and still achieve discrimination. When a similar attempt at data deletion was attempted for the realistic aircraft models it was found that only the first two harmonics could be deleted. This is not necessarily a negative result. The transients used to test discrimination were produced synthetically from scattering data at 2(2)20.0 MHz. It is clear from Tables 1, 2 and 3 that all the poles shown as dominant

θ=90, ϕ=0 θ polarization ($\times 10^6$)	θ=90, ϕ=0 ϕ polarization ($\times 10^6$)	θ=ϕ=90 θ polarization ($\times 10^6$)	θ=ϕ=0 ϕ polarization ($\times 10^6$)	average ($\times 10^6$)
$-6.33 \mp i91.7$	$-19.8 \mp i93.8$(d)	$-23.2 \mp i89.2$	$-19.6 \mp i94.2$(d)	$-19.7 \mp i94.0$
$-7.09 \mp i46.9$(d)	$-8.88 \mp i44.4$	$-6.94 \mp i46.8$(d)	$-4.26 \mp i45.3$	$-7.01 \mp i46.8$
$-2.79 \mp i131$	$-3.48 \pm i131$	$-.328 \pm i131$	$-4.28 \pm i131$	$-3.5 \pm i131$

Table 1. Natural Resonance of F-104 Aircraft Model.

θ=90, ϕ=0 θ polarization ($\times 10^6$)	θ=90, ϕ=0 ϕ polarization ($\times 10^6$)	average ($\times 10^6$)
$-13.2 \mp i63.3$	$-16.4 \mp i66.0$(d)	$-16.4 \mp i66.0$
$-10.9 \pm i43.7$(d)	$-9.08 \pm i42.7$	$-10.9 \pm i43.7$
$-18.6 \pm i131$	$-1.23 \pm i130$	$-9.9 \pm i130$

Table 2. Natural Resonances of F-4 Aircraft Model.

θ=90, ϕ=45 θ polarization ($\times 10^6$)	θ=90, ϕ=45 ϕ polarization ($\times 10^6$)	θ=0, ϕ=45 ϕ polarization ($\times 10^6$)	θ=0, ϕ=45 θ polarization ($\times 10^6$)	average ($\times 10^6$)
$-8.15 \mp i79.0$(d)	$-2.72 \mp i80.8$	$-9.30 \mp i79.7$(d)		$-8.72 \mp i79.3$
$-6.56 \pm i55.6$(d)			$-3.08 \pm i47.0$	$-6.56 \pm i55.6$
	$-9.81 \mp i66.8$(d)	$-8.04 \mp i64.7$(d)	$-10.2 \mp i67.1$(d)	$-9.35 \mp i66.2$
$0 \pm i131$	$-5.26 \pm i120$	$-.5 \pm i132$	$-1.44 \pm i132$	$-2.40 \pm i130$

Table 3. Natural Resonances of MIG-19 Aircraft Model.

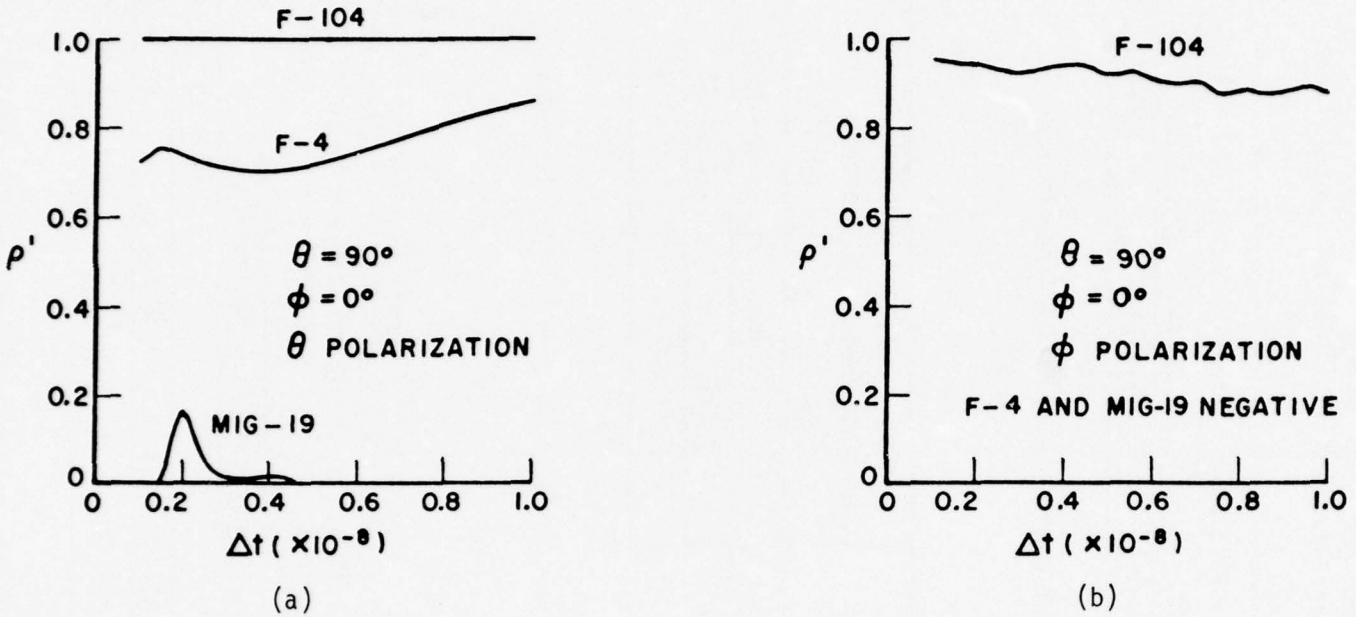

Figure 5. Discrimination test using measured ramp response of F-104 aircraft.

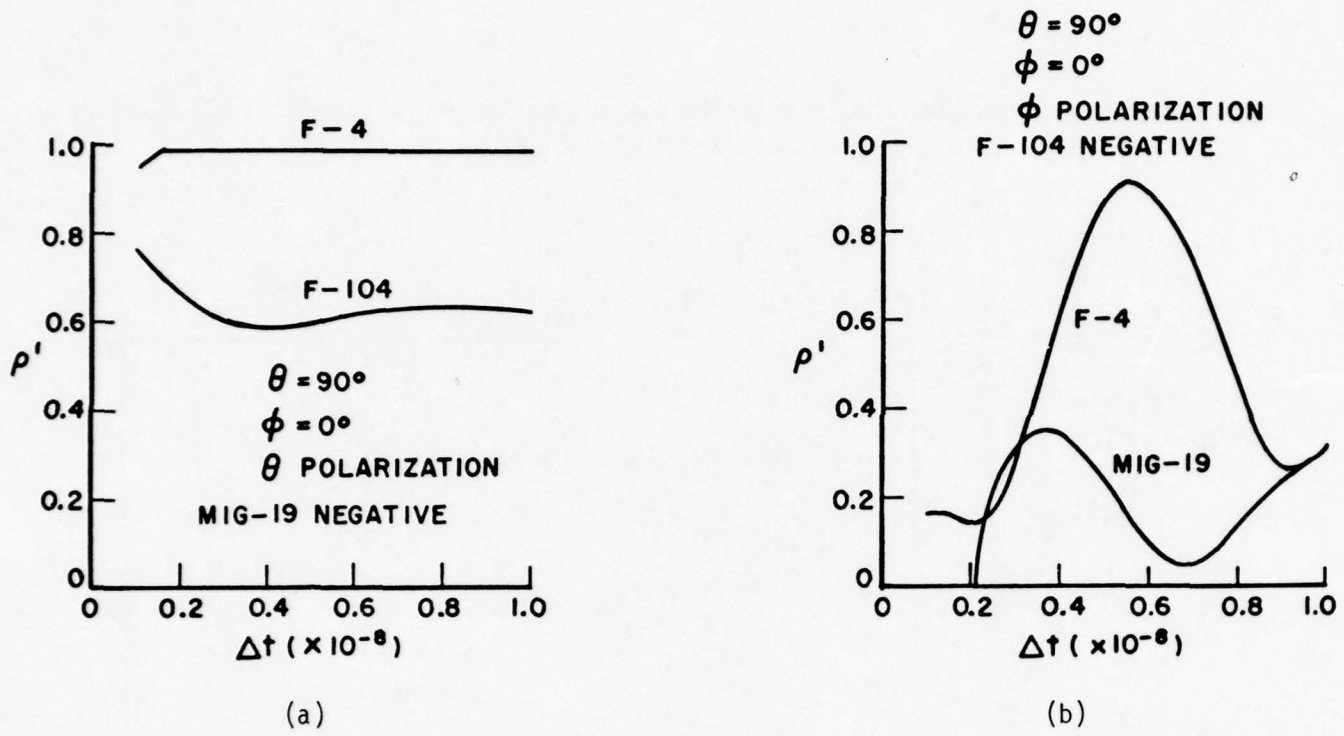

Figure 6. Discrimination test using measured ramp response of F-4 aircraft.

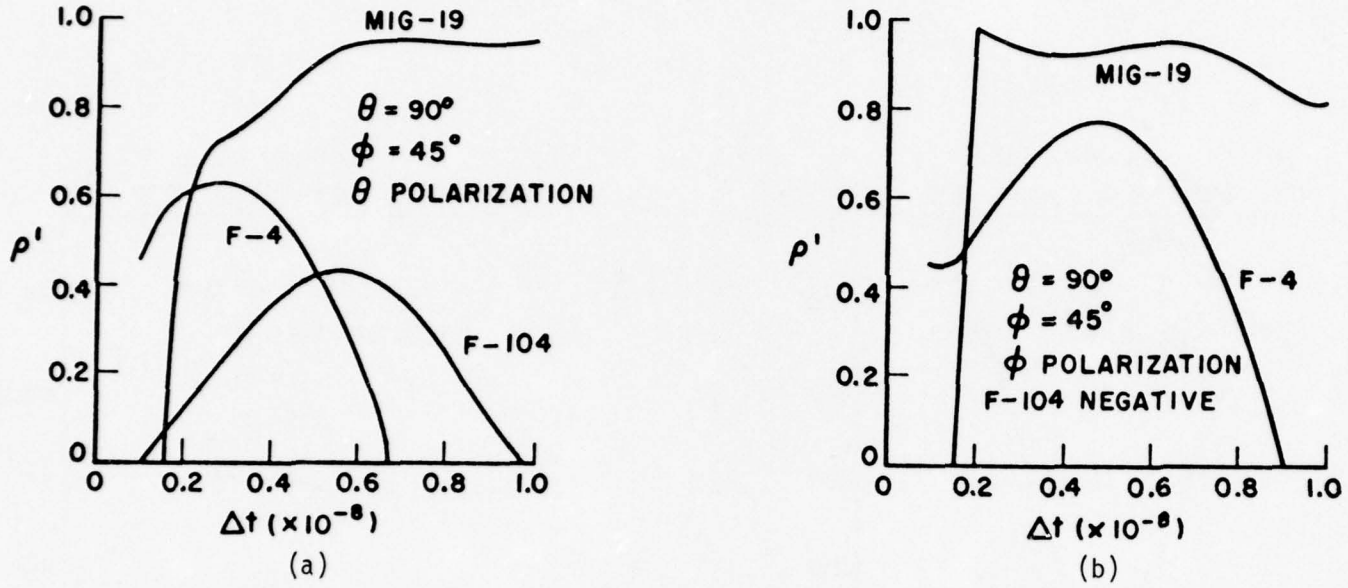

Figure 7. Discrimination test using measured ramp response of MIG-19 aircraft.

are excited on this span of excitation frequencies. However if the excitation frequencies had been concentrated near the oscillatory part of one resonance, say $130 \times 10^6/2\pi$ Hz, good discrimination may have been possible. This suggests that with the dominant poles of a class of radar targets known, it may be possible to tailor the interrogating signal waveform to exploit only certain of the pole locations. This would have certain disadvantages in terms of restricting the target orientations and radar polarizations for which the scheme will work. The interrogating signal however could be much simpler. This type of restricted target identification needs to be studied.

It was found (see Appendix) that when noise is added to the scattering data changes in the processing procedure were needed. First the discrimination quantity, unity minus the normalized squared error, was renormalized such that nominally only values between zero and one are obtained. The reason for this change is that with substantial noise even the desired curve became negative and uninterpretable. The simplified noise analysis described in the Appendix shows that the signal to noise ratio is most critical at the lowest harmonics. For this reason the ramp weighting was discarded and an inverse three-halfs weighting used instead. In addition, doubling of the signal to noise ratio at the first two harmonics was added. It can also be shown that when the difference equation, which is the heart of the predictor-correlator processor, always is used to predict future values from prior values then noise effects are magnified because the difference coefficients can become quite large. However, if the difference equation is normalized by the magnitude of the largest coefficient then the largest coefficient is unity. In this way a predicted value comes, in general, from both prior and future values. The effects of these various changes are illustrated in Figures 8, 9, 10 and 11 for realistic models of the F-4 and F-104 aircraft. In Figure 8 the aircraft are being viewed broadside to the bottom with polarization parallel to the wings, and the F-104 is the desired target. Two results are shown corresponding to noise to signal power ratios of 0.0 and 0.04. In Figure 8, a ramp weighting is still being used and the signal transmitter power is the same at each harmonic. Note that a sample increment of 0.048 seems to optimize the scheme in the presence of noise. In Figure 9 the configuration of Figure 8 is repeated but this time a three-halves weighting of the interrogating signal is used and the signal to noise power is doubled at the first two harmonics. Here, noise to signal powers of 0.0, 0.04 and 0.16 are shown. In Figure 9 it is seen that the optimum sample intervals of 0.048 remains and that increasing the noise to signal power by a factor of four has little effect. In each case good discrimination is achieved. In Figure 10, the scheme of Figure 9 is repeated but this time for polarization parallel to the fuselage of the aircraft.

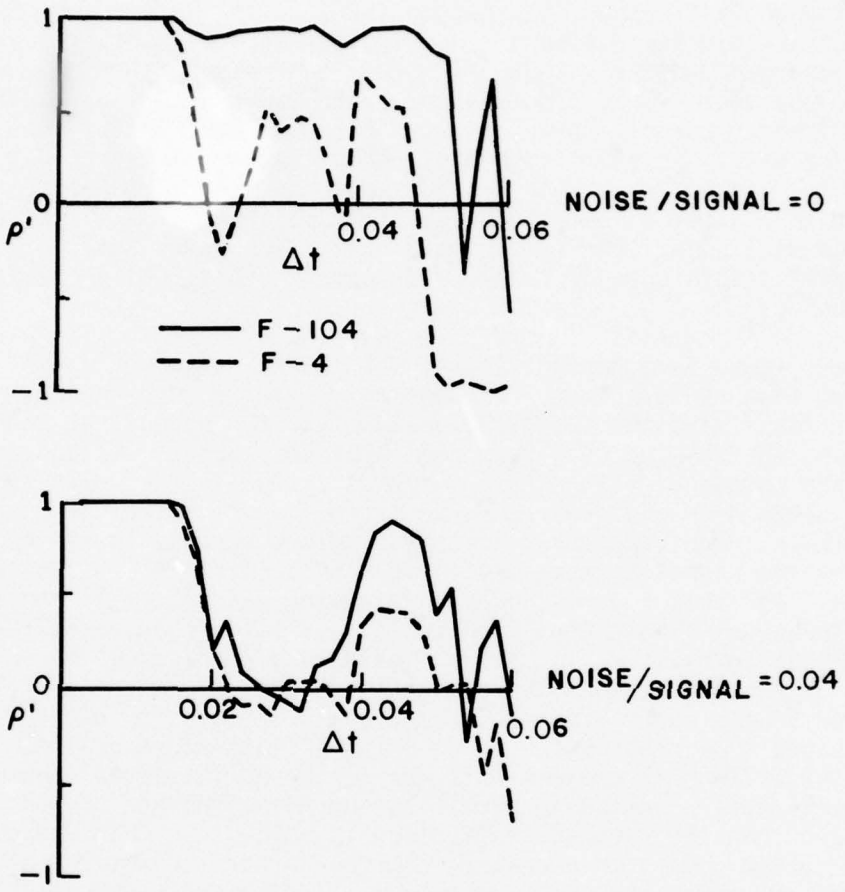

Figure 8. θ=90, ϕ=0, ϕ-polarization; input poles: F-104, ramp response; (S/N) of all harmonics equal.

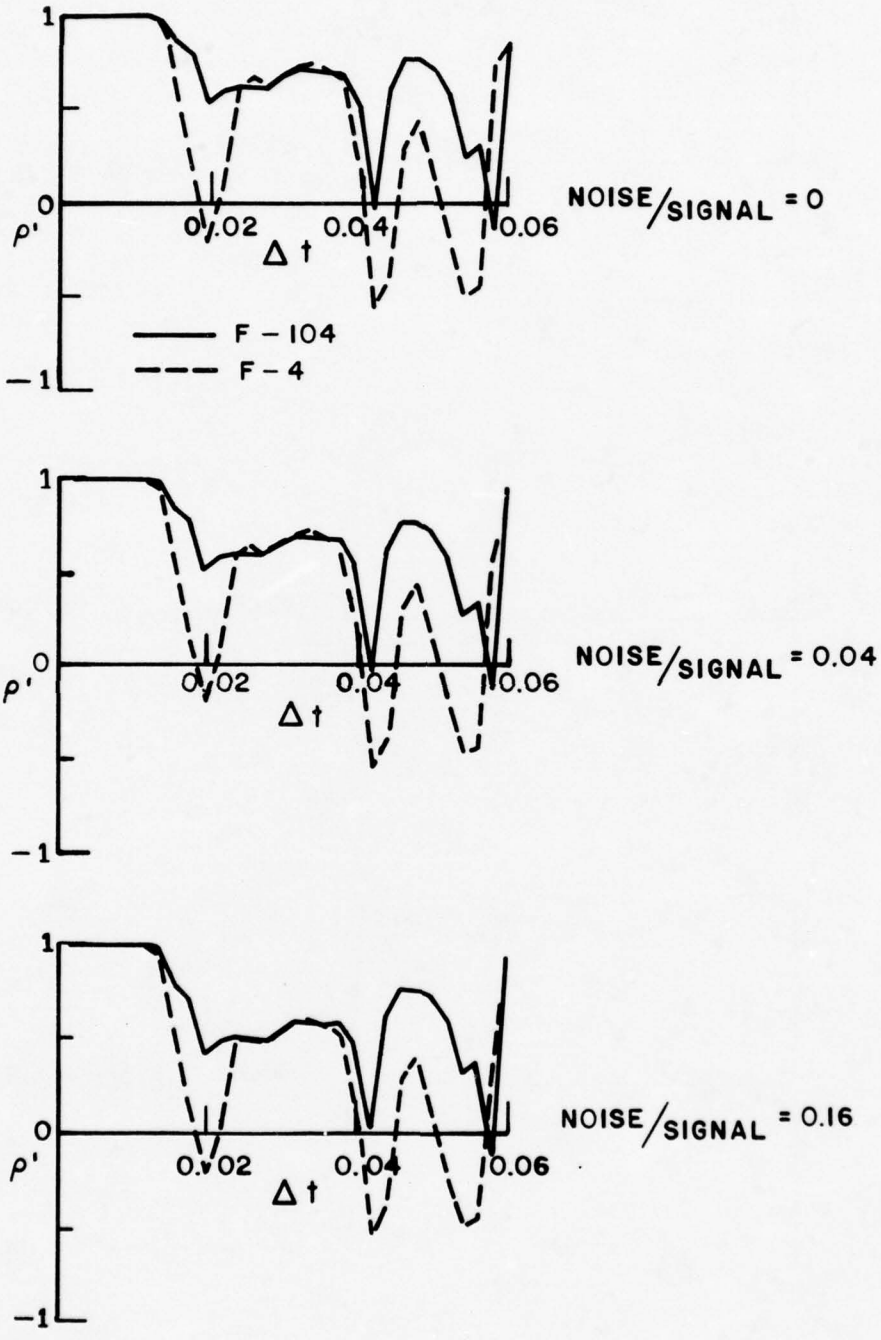

Figure 9. θ=90, ϕ=0, ϕ-polarization; input poles: F-104; $n^{-3/2}$ weighting; (S/N) doubled for harmonics 1, 2.

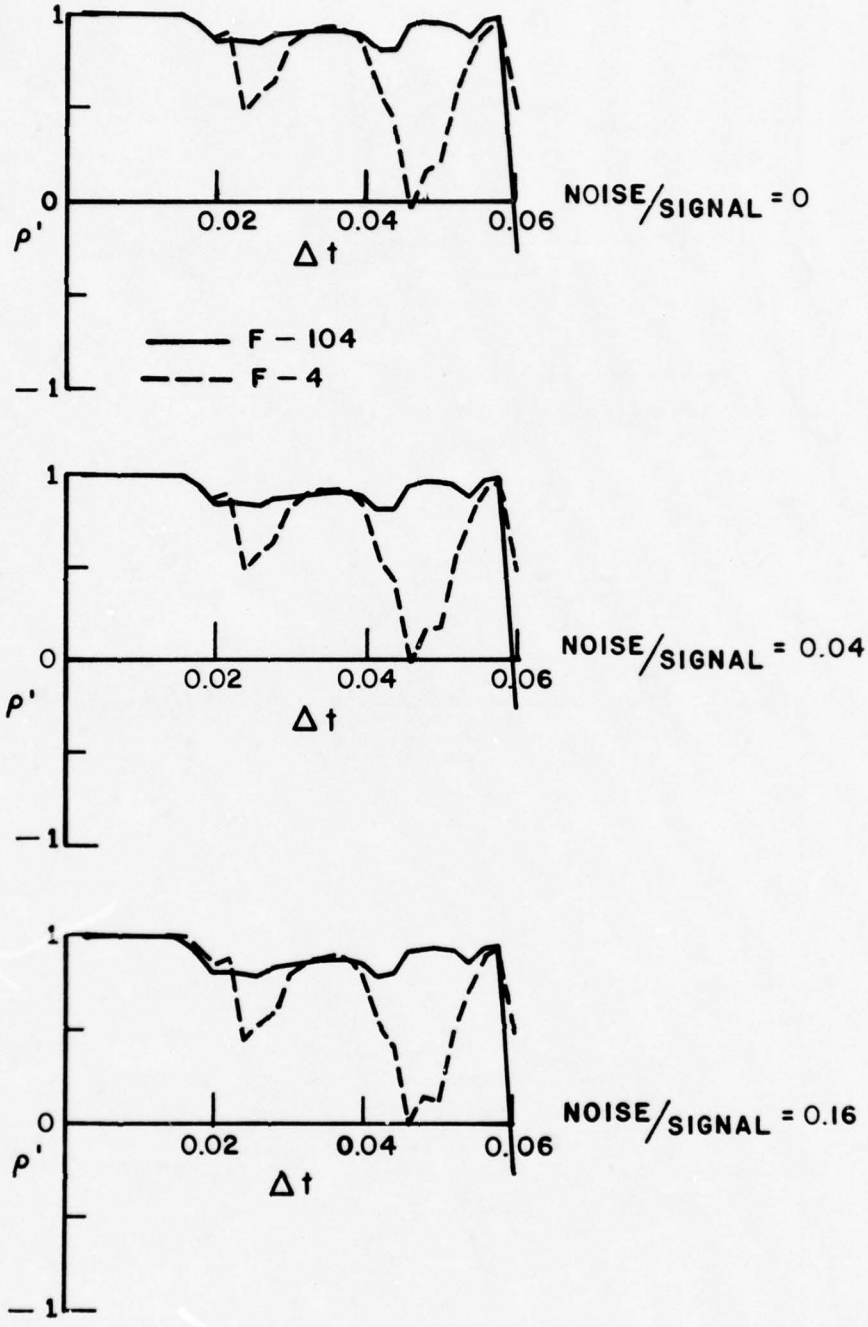

Figure 10. θ=90, ϕ=0, θ-polarization; input poles: F-104; $n^{-3/2}$ weighting; (S/N) doubled at harmonics 1, 2.

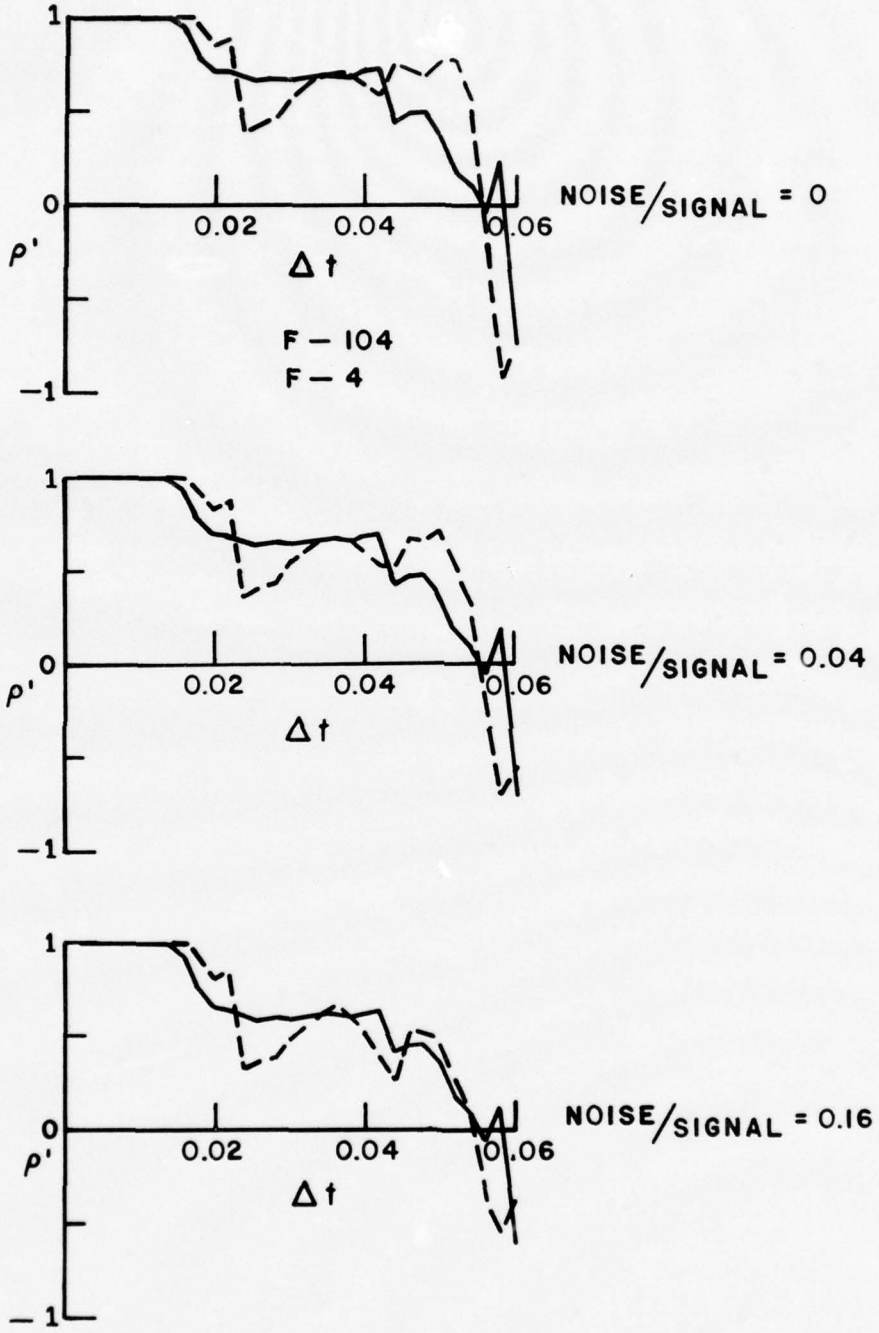

Figure 11. θ=90, φ=0, θ-polarization, input poles: F-4; $n^{-3/2}$ weighting, (S/N) doubled at harmonics 1, 2.

The optimum sample interval remains the same and increased noise power has very little effect. In Figure 11 the process is reversed for the same target orientation as Figure 10 and the F-4 aircraft is the desired target. Here we see that while the optimum sample interval is the same, increased noise power appears to begin to negate the discrimination scheme. This is not unexpected. The target discrimination scheme is target orientation dependent and at particular target orientations may be more noise sensitive than at others. The results in Figures 8 through 11 are extremely encouraging. The ability to fix the sample interval for a given target and an indication of insensitivity to noise are very important results.

It has also been demonstrated that a rational function fit of scattering and/or admittance data at a regular grid (in the complex frequency plane) of real and complex frequencies can be used to extract the target poles. The process is not precise as inexact pole locations are sometimes obtained, but no evidence of the erroneous poles sometimes given by the Prony method have been obtained. For complicated target geometries the rational function fit could be used first to provide starting points for the iterative search procedure. This procedure has no application to measured data.

III. CONTROL OF NONSPECULAR ELECTROMAGNETIC SCATTERING

The GTD diffraction coefficients can be used to demonstrate that edge diffraction scattering is largest for the trailing (leading) edge when the incident wave is vertically (horizontally) polarized. Using this concept as a guide we proceeded to study techniques for the reduction of RCS caused by edge diffraction.

A. Trailing Edge RCS Reduction for Vertically Polarized Waves

First, attention was focussed on the trailing edge and is reported in detail in [11]. A number of wedge geometries, strip geometries and wing foils were considered. The means of loading these 2-D geometries consisted of inserting a strip (or strips) of surface impedance on the conducting surfaces. As observed in the introduction, mathematical modeling of these 2-D geometries involved conventional moment method (mm), Geometrical Theory of Diffraction (GTD) and a new hybrid solution. It was indeed demonstrated that the back scattered fields from the trailing edge could be controlled by such surface impedance strips.

One of the original goals of this research was to use an antenna with a properly designed impedance at its terminals. For the trailing edge the antenna took the form of a slot placed near the trailing edge. This was modeled using a wire grid moment method solution as shown in Figure 12 where the slot terminals are indicated by abc. The echo area reduction achieved for this flat plate is given in Figures 13 and 14. For Figure 13, the length $L = 0.6\lambda$ and it is observed that several orders of magnitude reduction have been obtained for the trailing edge condition, i.e., for $\theta > 90°$. Figure 14 shows the same result for the case where $L = \lambda$ (labeled open circuit one slot). When a second slot is introduced on the other side of the plate RCS reduction is achieved for the complete pattern. Thus demonstrating that the slot near the trailing edge can effectively reduce the nonspecular scatter from edge diffraction for vertical polarization. This is effective over at least a two to one frequency band. This band could be increased if the slot length was made equal to the length of the edge of the plate. Further it is hypothesized that the slot need not be cut into the plate but could be simply an insulated wire placed over the load. The important factor should be the means in which the load impedance is introduced. If it is connected as in Figure 12 then the slot case occurs. The case for a different load position results in a folded dipole configuration to be discussed later. The impedance required for optimum RCS reduction for the case of Figure 12 is shown in Figure 15. This is probably not a physically realizable load but the same techniques outlined in the next section should be applicable to this slot geometry. This has not been verified however at this time.

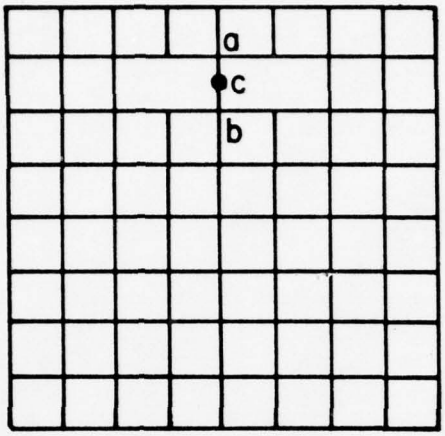

Figure 12. Conducting wire grid model of a half-wavelength long slot in a one wavelength square conducting plate.

B. Leading Edge RCS Reduction for Horizontally Polarized Waves

As in the case just discussed, a substantial research effort focussed on the reduction of RCS caused by leading edge diffraction for horizontal polarization using 2-D geometries. In particular, wing foil geometries were of prime interest. The details are reported in References [12,13]. This then lead to consideration of the folded dipole geometry.

C. Control of Nonspecular Electromagnetic Scattering

As shown in Figure 16, a thin square conducting plate slotted on one side is modeled with a wire-grid structure. Lumped impedances of values Z_1 and Z_2 are inserted on the slotted side. The purpose here is to optimize the impedances Z_1 and Z_2 such that significant reduction of the backscatter from the slotted plate can be achieved at near grazing incidence with electric field polarized parallel to the slot. Although there are three lumped impedances (Z_1, Z_2, Z_2), the formulas for the case of two lumped impedances derived in the previous section can still be used if the symmetry property of the structure is employed.

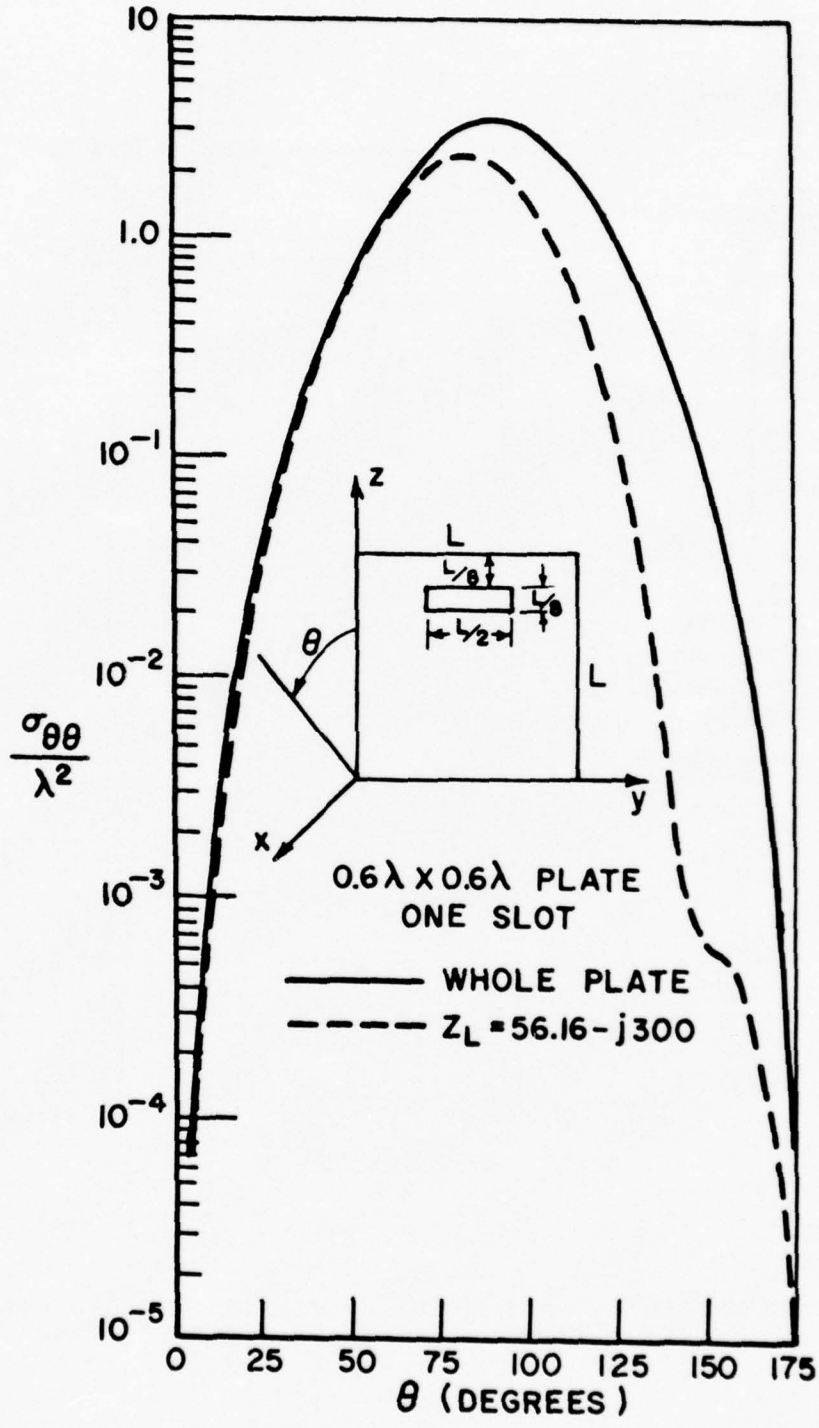

Figure 13. Use of a loaded slot for reduction of an edge diffracted field from a flat plate.

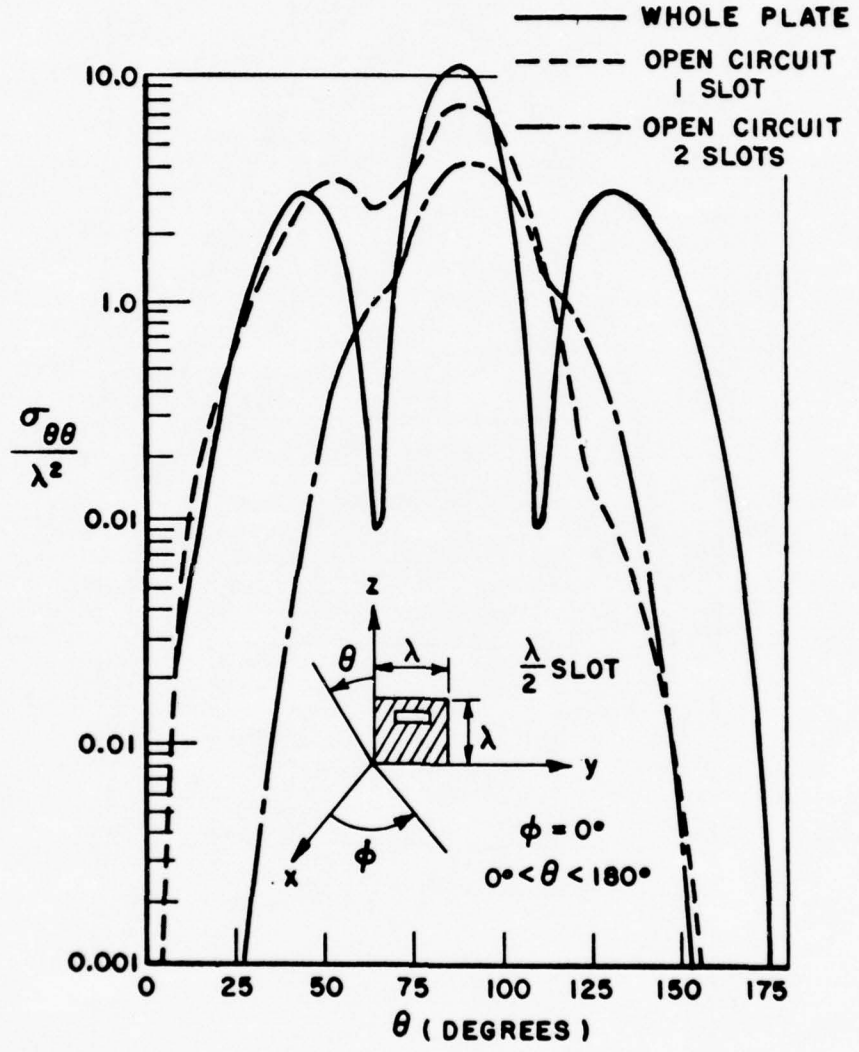

Figure 14. Backscattering cross section ($\sigma_{\theta\theta}/\lambda^2$ for the $\hat{\theta}$ polarization) of a square conduction plate with one and two slots.

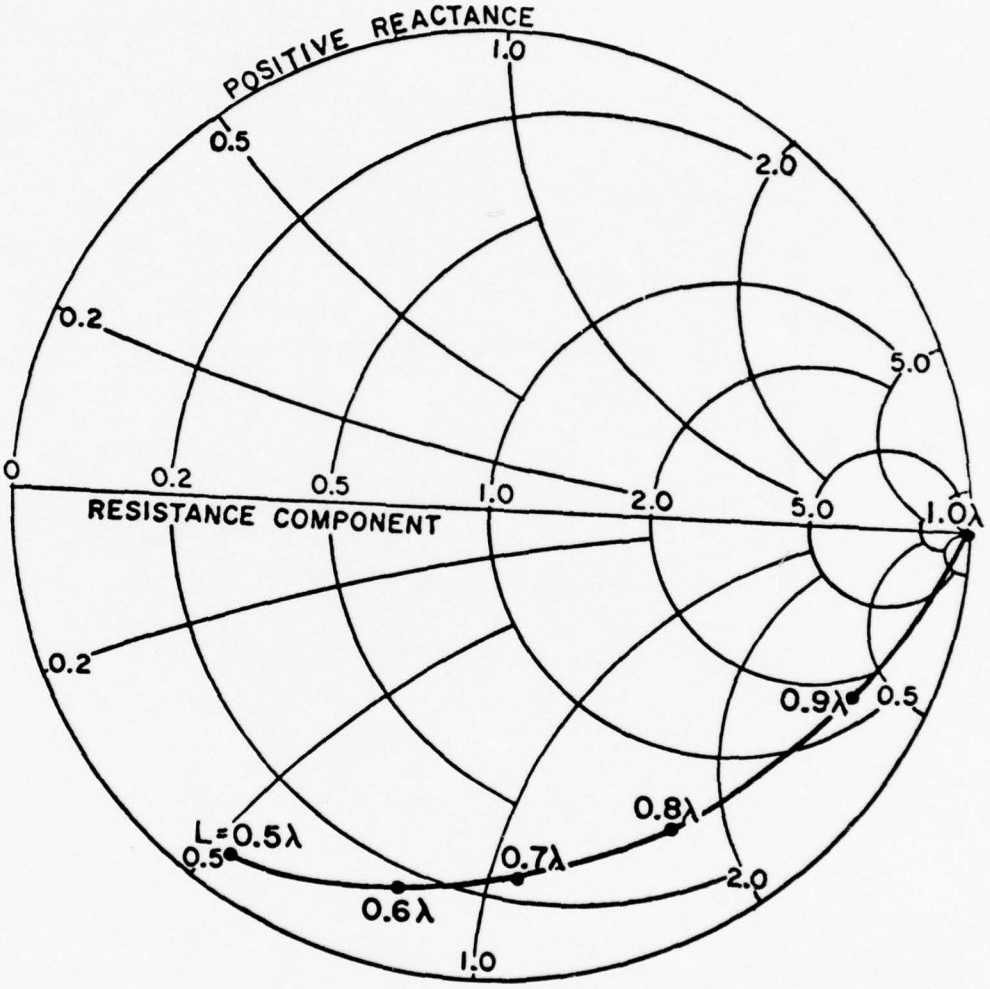

Figure 15. Load impedance required for reduction of wedge diffracted backscattered fields.

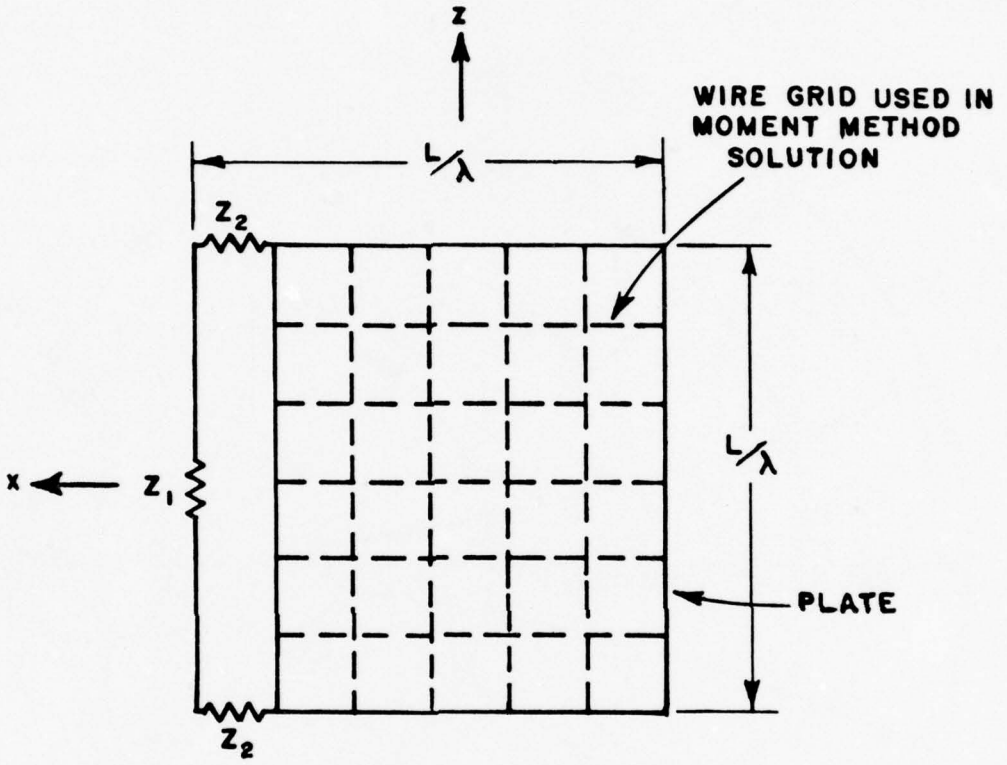

Figure 16. Wire grid model of folded dipole geometry.

From folded dipole theory, Z_2 is chosen to be pure reactive. However, Z_1 can have resistance. We first calculate the antenna impedances $Z_{a1}(o,o)$, $Z_{a1}(o,Z_2^x)$, $Z_{a2}(Z_1^x,o)$ and the backscattered fields $E(o,o)$, $E(o,Z_2^x)$, $E(Z_1^x,o)$, $E(Z_1^x,Z_2^x)$ using a computer program developed by Richmond [5]. Then varying the values of Z_1 and Z_2 and calculating the backscattered field $E(Z_1,Z_2)$ using the formulas derived in the previous section, we obtain a figure of merit as the sum of the echo areas at ϕ=0°, 10°, 20°, 30°, 40°. The computer is programmed to select the load impedances yielding the smallest figures of merit. The optimal values of Z_1 and Z_2 are then determined. Typical results are shown in Figures 17, 18 and 19. For low frequencies (below that frequency for which an edge is of the order of $\lambda/2$), reduction for the complete pattern is obtained. For higher frequencies substantial reduction is

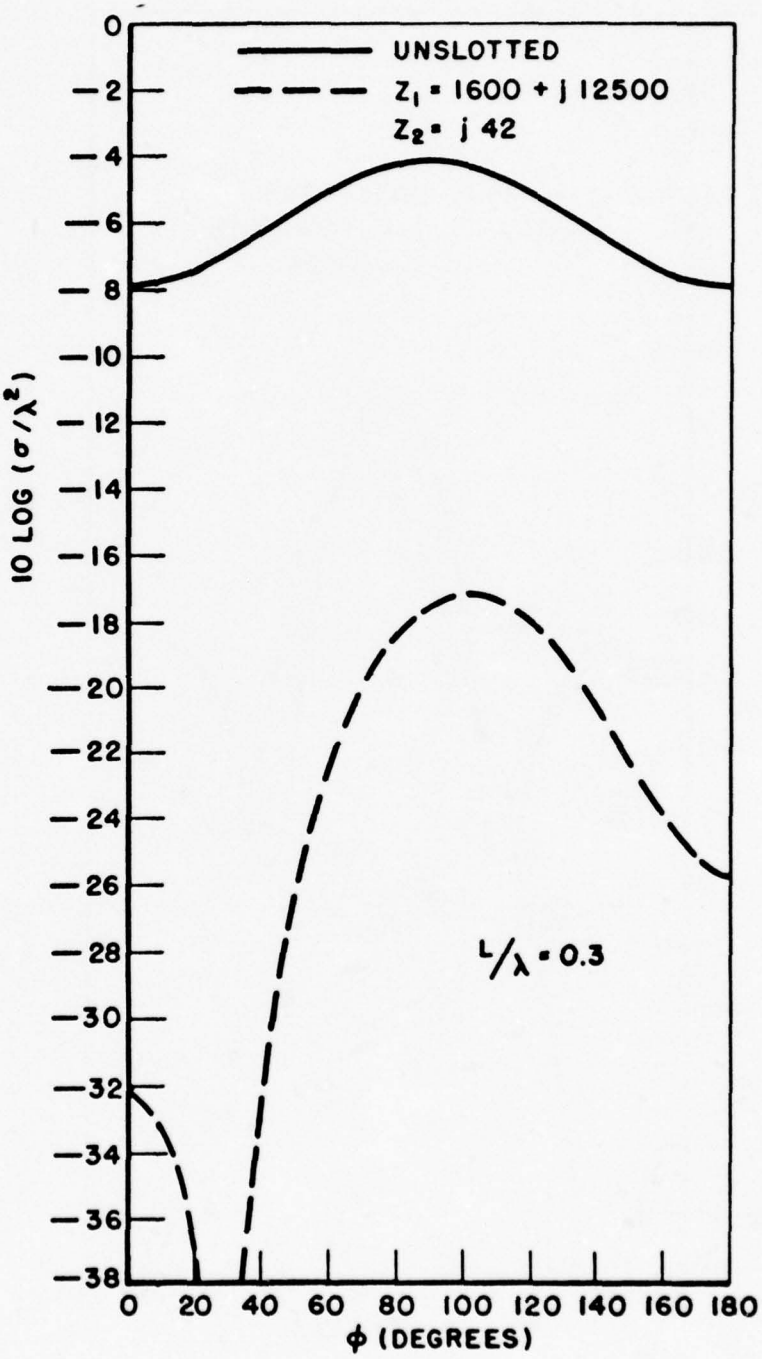

Figure 17. Backscatter reduction for parallel polarization.

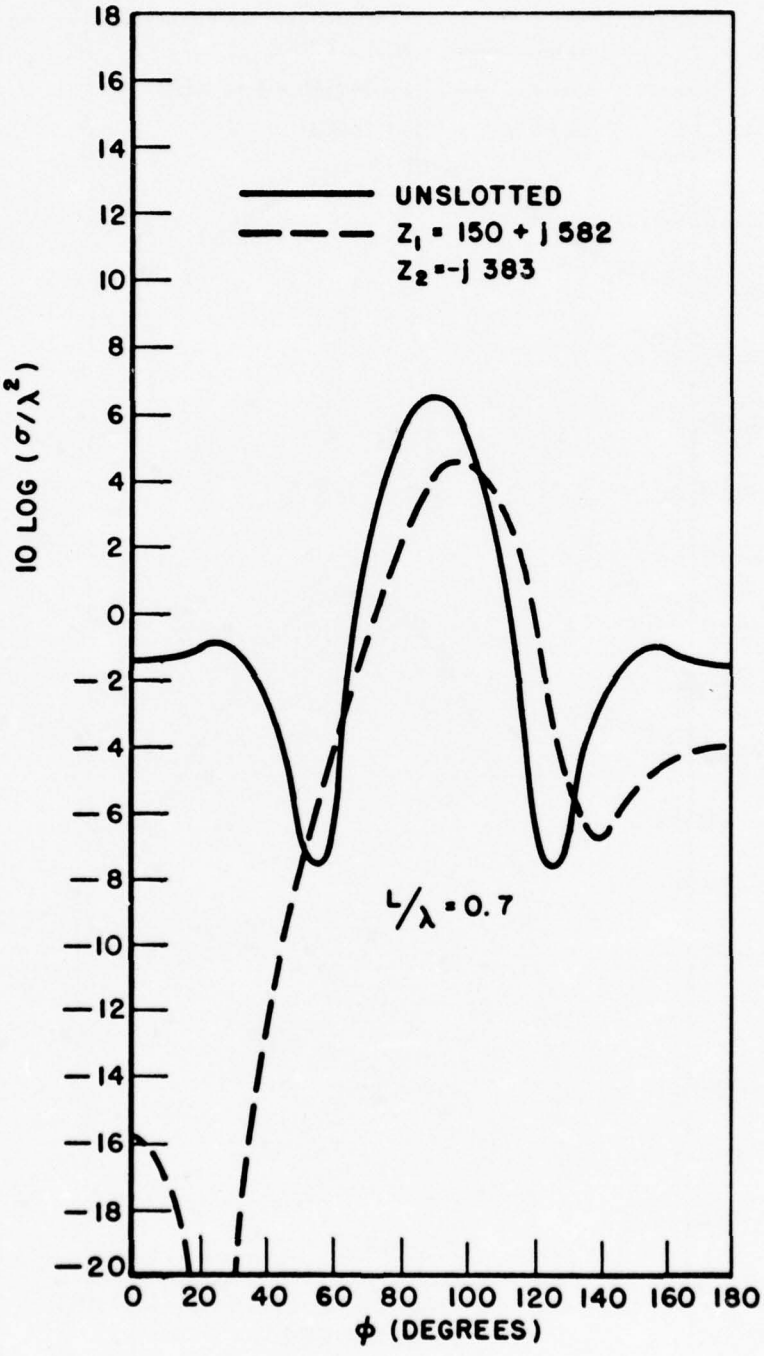

Figure 18. Backscatter reduction for parallel polarization.

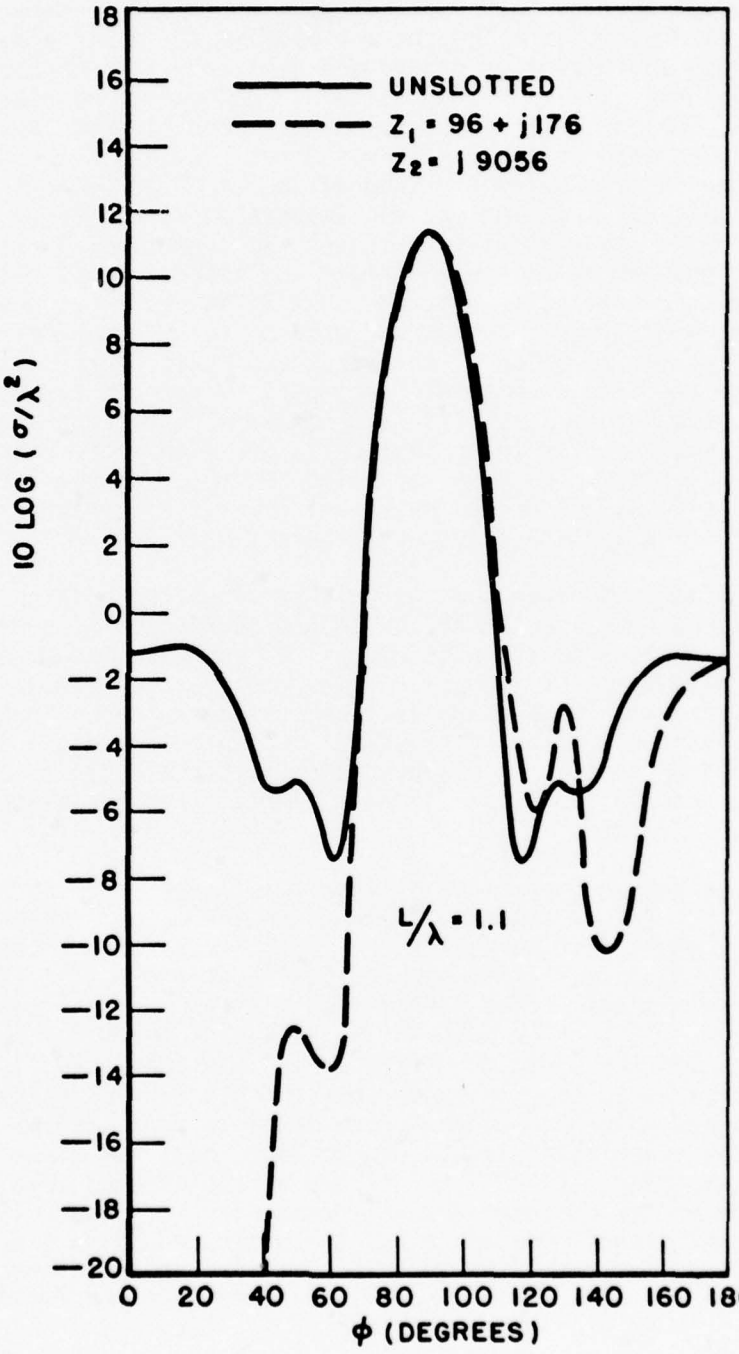

Figure 19. Backscatter reduction for parallel polarization.

achieved up to almost 50° from grazing incidence. One exception occurs for the frequency where the edge length is 0.9λ. Here almost no reduction in RCS is obtained but the endfire RCS is already low. Both echo areas for unslotted plates and slotted plates with optimal Z_1 and Z_2 are presented. The reduction of backscatter at near grazing incidence can be achieved for plate sizes ranging from $L/\lambda = .1$ to $L/\lambda=1.4$. The size of $L/\lambda=1.4$ is not a restriction on the target size but merely one introduced by the core of the computer being used to make these computations. The optimal impedances Z_1 and Z_2 for minimizing the backscatter at near grazing incidence are summarized in Figures 20 and 21. The problem of how to implement the impedances is not dealt with at this time. However it is observed that Z_2 is the impedance required to reflect an open circuit across the antenna for the asymmetrical current mode at the position of the input terminals of the folded dipole. This could be realized at a single frequency by placing a short circuit (shorted diode) across the antenna at the proper place. The impedance Z_1 would appear to be physically realizable over most of the frequency band. Thus, the echo reduction suggested can be achieved using an adaptive system where the frequency of the incoming radar is sensed and the appropriate diode would be activated.

With optimal impedance loading which reduces the backscatter at grazing incidence we expect that the induced current will redistribute itself on the plate. As shown in Figures 22 and 23, the current on an unslotted square plate of size $L/\lambda=.2$ induced by a plane wave of parallel polarization at grazing incidence is compared to that induced on a plate of the same size with optimal impedance loading. The change of the induced current at the leading edge (slotted edge) is large. The total current in the z-direction is reduced when the plate is loaded with optimal impedances.

Impedance loading may find applications in the study of target discrimination. Target discrimination using the natural resonances of a target as important parameters has been discussed earlier. Here it is interesting to ask if impedance loading of a target will alter the natural resonances of the target drastically. For the square plate studied in this section the dominant natural resonances can be obtained as follows. With the unslotted plate Prony's method is applied to the endfire backscattered ramp response obtained via Fourier synthesis and the dominant natural resonances are found to be $(-.515 \pm j1.91)c/L$ where c is the velocity of light (Figure 24). Next the plate is slotted and a fixed impedance $Z_1=200\Omega$ is inserted at the slotted edge. A slight change in the dominant natural resonances is found (Figure 25). At the dominant natural resonances of the unslotted plate the size of the plate is approximately $L/\lambda=.3$. If optimal impedances are obtained at this frequency which, from Figure 17, are found to be $Z_1=1600+j12500$, $Z_2=j42$ which can be made of some values of resistance and inductance, and if the values of resistance and inductance are kept constant, then the endfire backscattered ramp response is as shown in Figure 26.

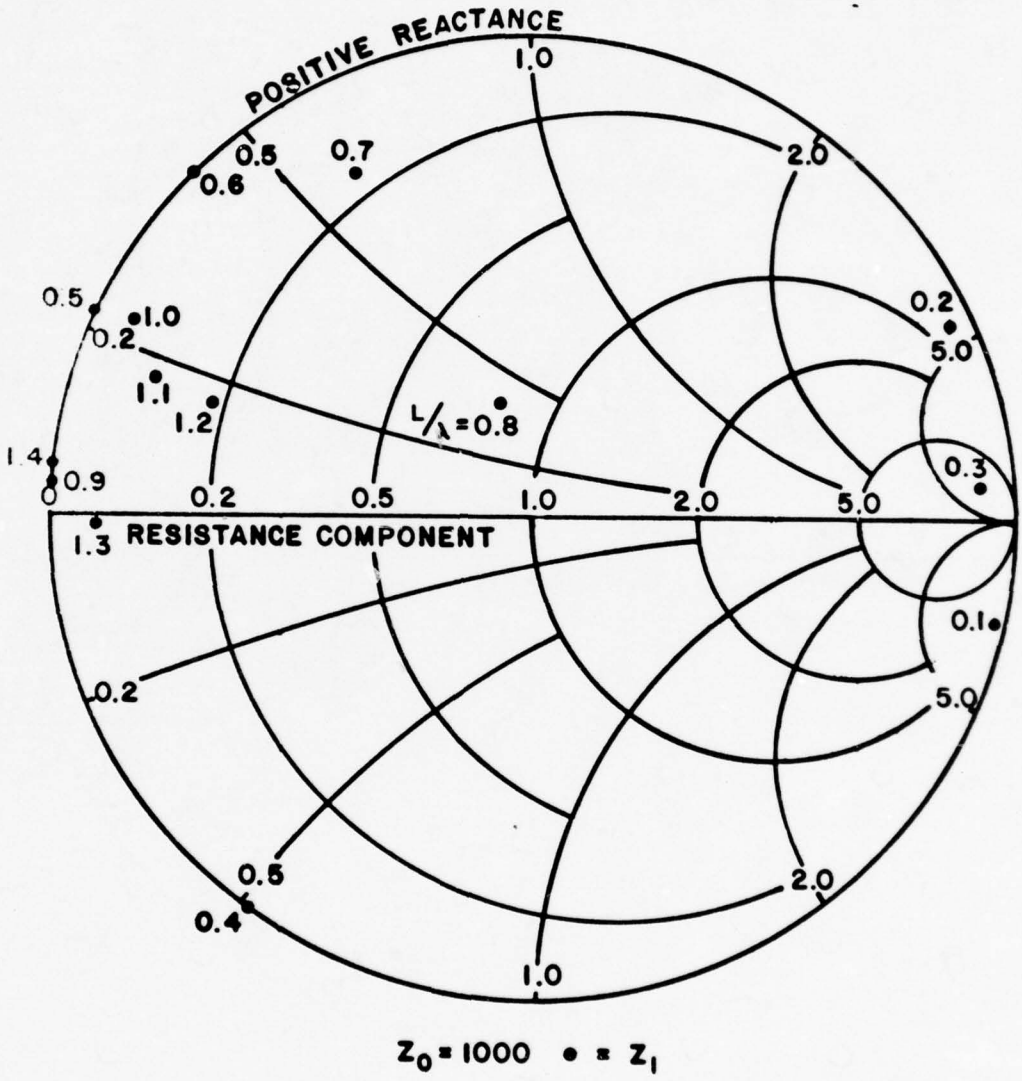

Figure 20. Values of Z_1 as function of L/λ.

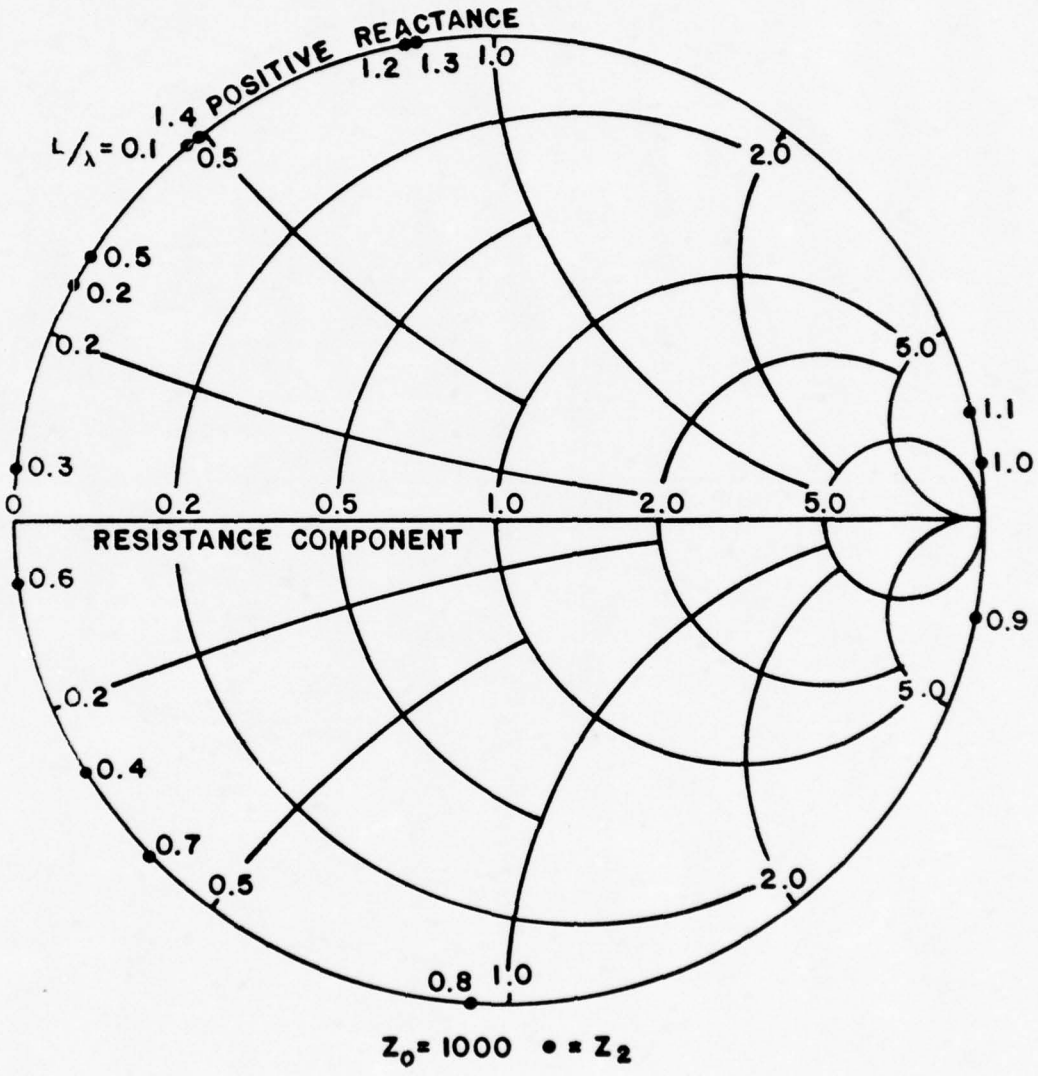

Figure 21. Values of Z_2 as function of L/λ.

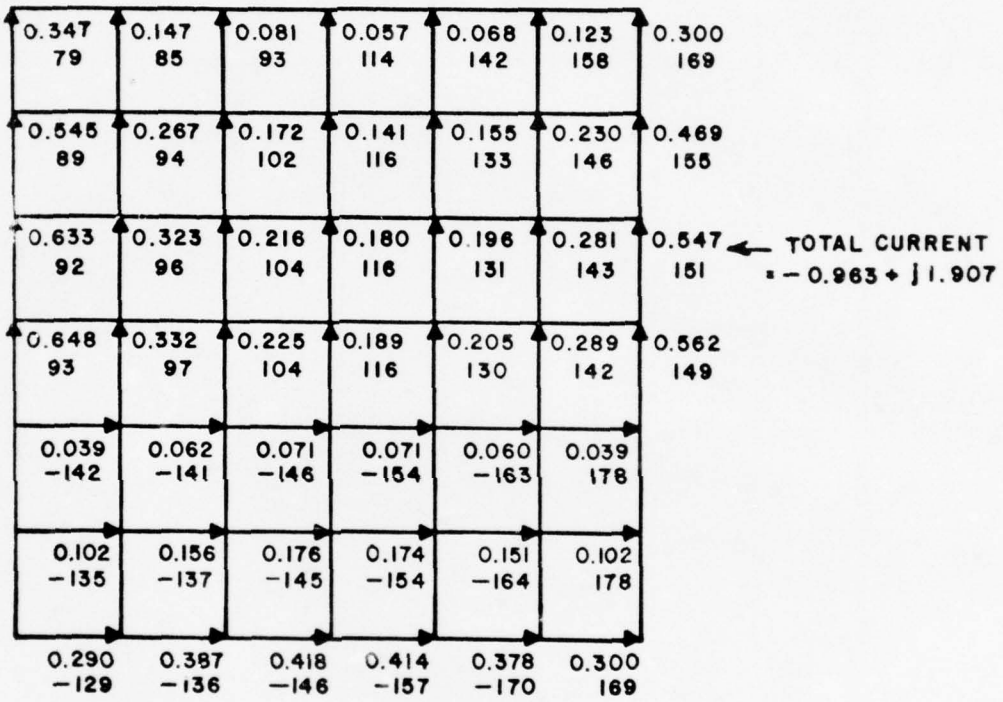

Figure 22. Current on a square plate of L/ =.2 induced by a plane wave at grazing incidence. The upper number is the amplitude and the lower number is the phase in degree.

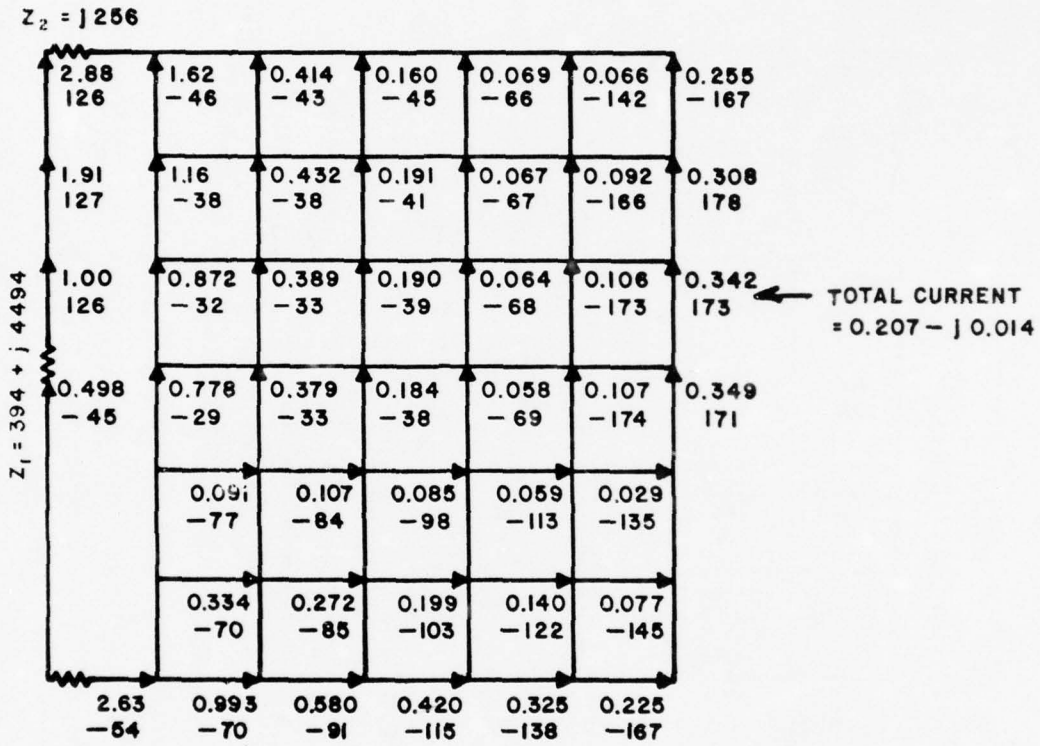

Figure 23. Current on a square plate of L/λ=.2 with optimal impedance loading induced by a plane wave at grazing incidence. The upper number is the amplitude and the lower number is the phase in degree.

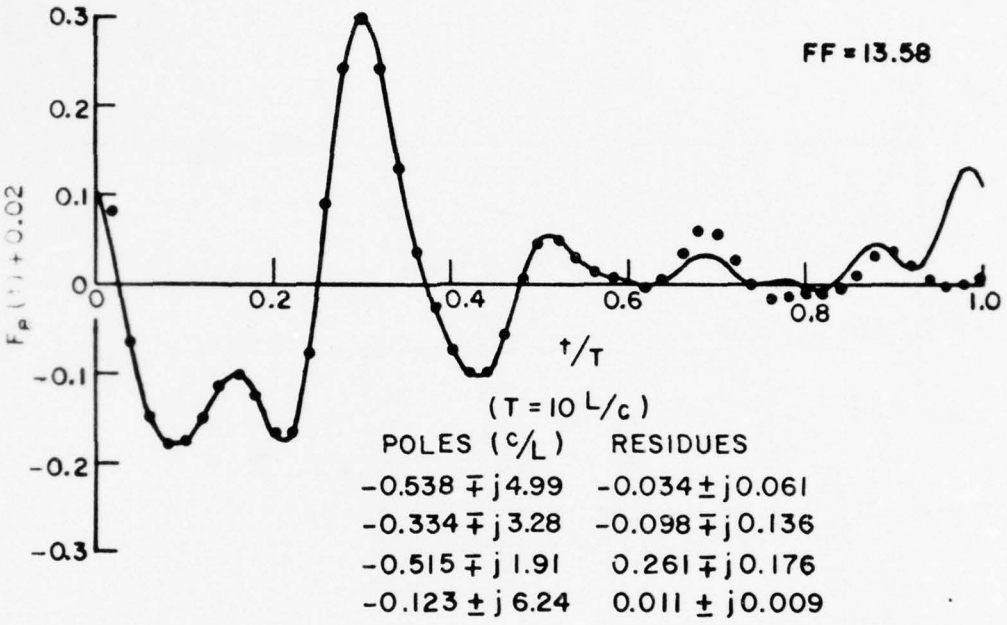

Figure 24. Endfire backscattered ramp response of a square plate.

The dominant natural resonances have a much larger change from those of an unslotted plate. It should be noted that the ramp responses as shown in Figures 24 through 26 must be divided by the factor (FF) to obtain the true ramp responses. For comparison, the corresponding broadside backscattered ramp responses are shown in Figures 27 through 29. Comparing the first negative swing in Figures 27 through 29, it is seen that impedance loading has little effect on the specular scattering. This brief investigation is by no means complete, but does show that impedance loading technique for controlling nonspecular scattering may also find applications in target discrimination.

Substantial reduction of the scattered fields from a leading edge for an incident horizontally polarized wave has been achieved theoretically over a broad frequency band using an impedance loaded folded dipole concept. There are a series of additional steps that could be implemented to extend these results to convert them from a basic concept to a practical result. These are listed below:

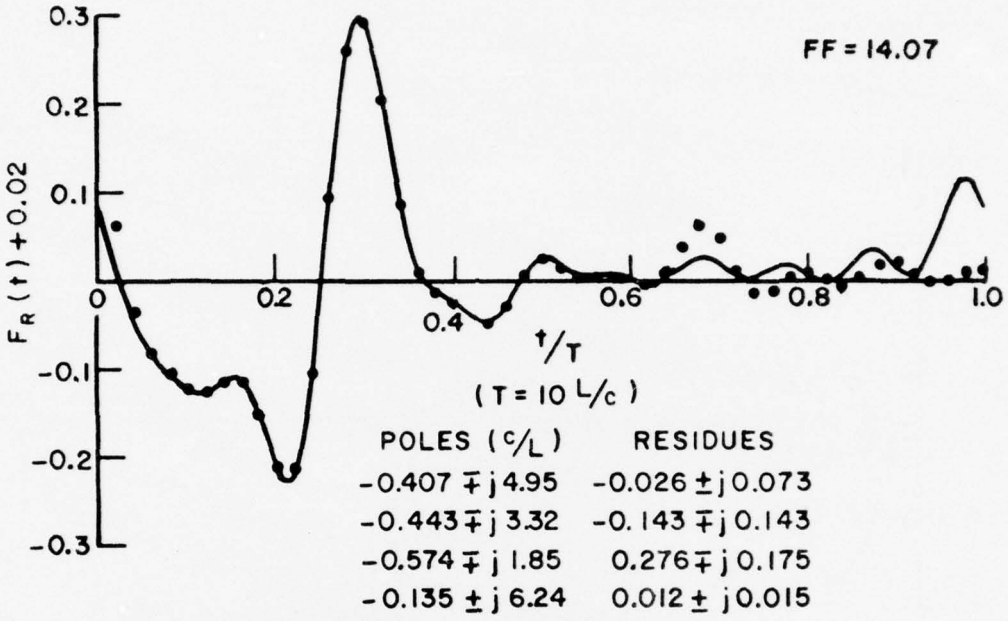

Figure 25. Endfire backscattered ramp response of a slotted square plate loaded with Z_1=200Ω.

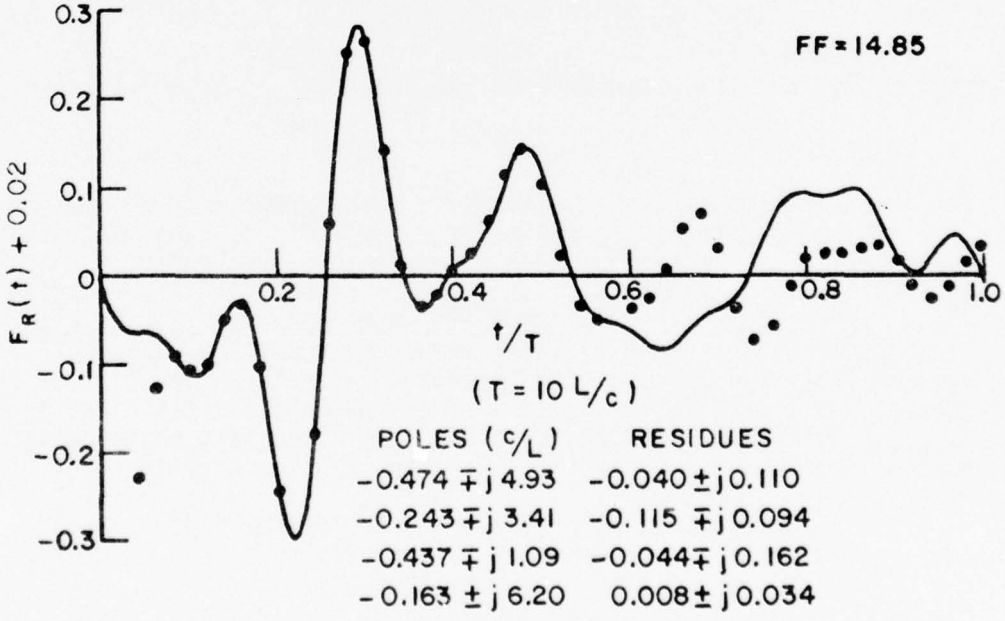

Figure 26. Endfire backscattered ramp response of a slotted square plate loaded with impedances which are optimal at the frequency where L/λ=.3.

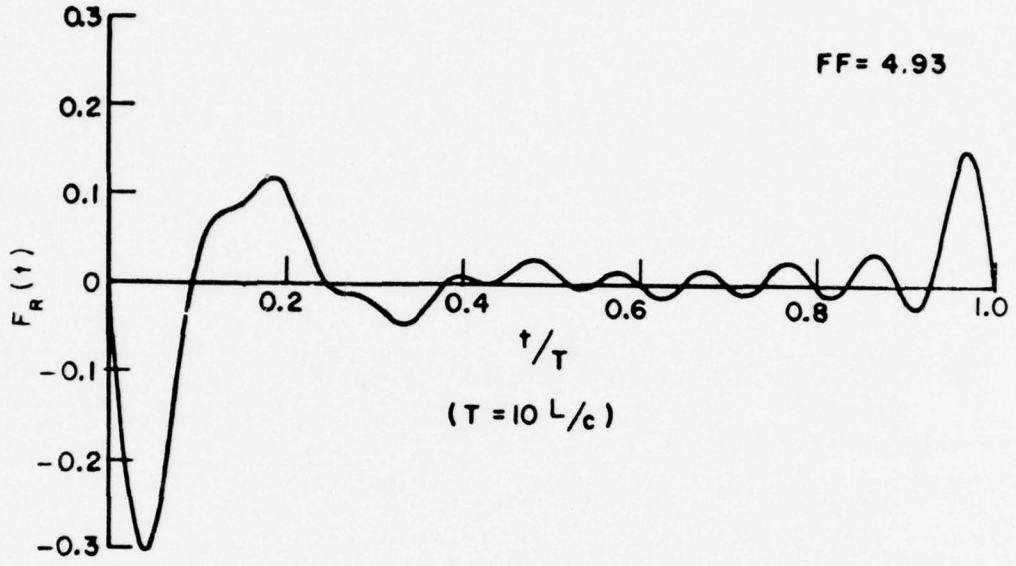

Figure 27. Broadside backscattered ramp response of a square plate.

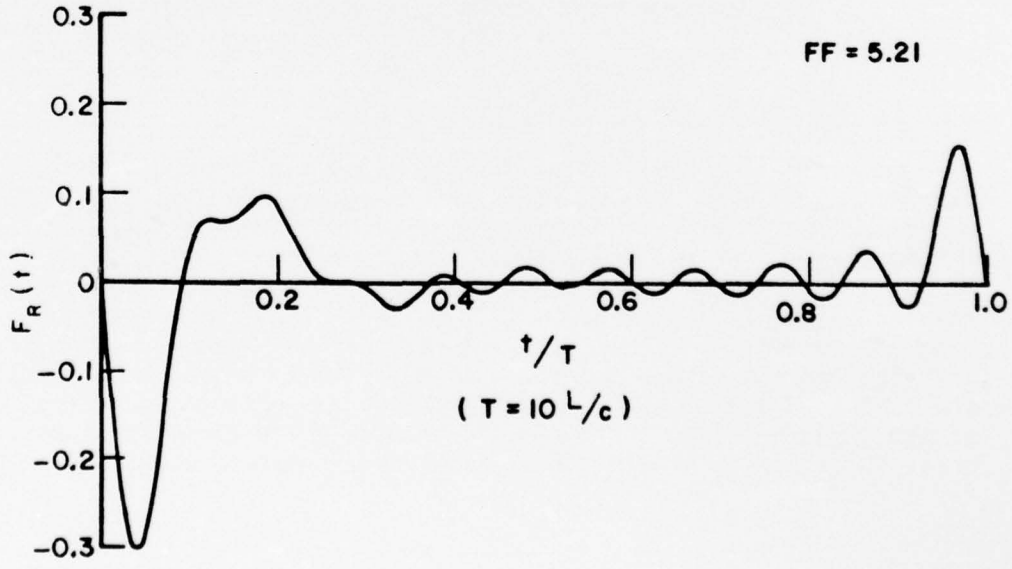

Figure 28. Broadside backscattered ramp response of a slotted square plate loaded with Z_1=200Ω.

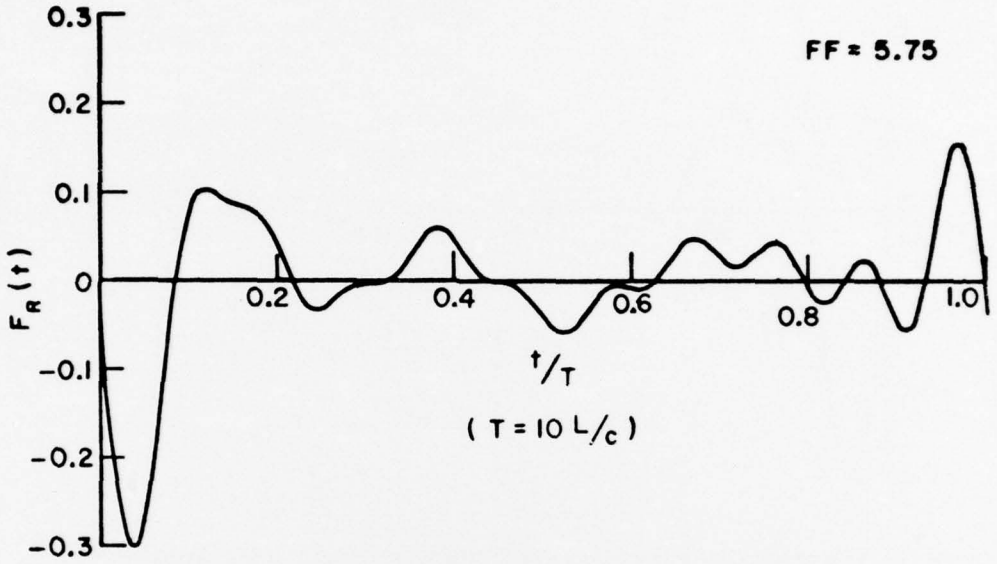

Figure 29. Broadside backscattered ramp response of a slotted square plate loaded with impedances which are optimal at the frequency where $L/\lambda=.3$.

1. Parameters of Loaded Slots and Folded Dipoles

The previous studies have shown good reduction of RCS for trailing edges using loaded slots over a reasonable band, but such reduction over a very broad band was obtained using the loaded folded dipole. It is believed that the bandwidth for RCS reduction can be increased by increasing the slot length to correspond to the length of the edge. At this time, there should be some improvement by further studying all of the parameters of both the slot and the folded dipole to optimize both the RCS reduction, and bandwidth and to minimize any problems inherent in the design of the impedance loads. This could be done using the flat plate model in conjunction with the existing moment method solutions.

2. Flat Plate Models of Aircraft

To date in these studies simple square flat plates have been used to model the edges. It is desirable to better model an actual aircraft and this is to be done using a flat plate version of an aircraft. A moment method solution for such an aircraft model is to be obtained with our loaded antenna geometries placed parallel to the edges of the wings. In the low frequency regime this model is a valid representation to the aircraft. This is true as long as the wing thickness is small in terms of wavelength. For higher frequencies, a better model of the aircraft may become important and the first important change in dimension would be the length of the wing. This may be appropriately treated by multiple loading as is to be discussed in the next section. Also a model of the aircraft that would include wing thickness, etc., may be introduced composed of a wire grid representation of the aircraft surface.

3. Multiple Antenna Loading

In our previous studies, we have used loaded slot and loaded folded dipoles for RCS control. The question now being raised is can multiple loading be introduced to combine both the loaded slots and loaded folded dipoles in one structure since the terminals of the folded dipole are taken across the conductor forming one component of the folded dipole whereas the terminals of the slot are taken across the slot. Thus, while both sets of terminals occur at the same position, the loading would be in series and in shunt, and the shunt load would have no control on the symmetrical folded dipole antenna currents, etc.

In addition, a multiple set of terminals spaced along the length of the antenna should be considered. This should make it practical to use these impedance loading concepts on longer structures or at higher frequencies than is thus far contemplated. The method of approach parallels that already used. We could modify the moment method solution for the analysis of elongated plates in lieu of the present square plate and introduce the load impedance at the appropriate points.

4. Experimental Verification

All of our results to date have been based on computations. It is important to seek further techniques for reducing this procedure to practice. Because of the difficulty of constructing impedances at microwave frequencies where our radar systems now operate, it would be beneficial to consider implementing this impedance loading concept at lower frequencies which in turn would also be more compatible with practical operation. Therefore we envision combining the concept of a transmission line radar range with short pulse techniques. We have

at present in operation broad band balanced systems that could be used to launch a pulse on a parallel line transmission line. A sampling oscilloscope would act as a receiver. The only major task would be to protect the sampling diodes from the incident pulse and there are several ways to achieve this type of operation. The means of operation would consist of gating the received scattered pulse and using existing FFT routines on our computers to obtain the back scattered field through the desired region of the spectrum. For the transmission line excited in the balanced TEM mode, the fields in the region between the lines will closely resemble a plane wave. This should be a valid representation for plate structures at near grazing incidence.

5. Synthesis of Impedance Load z_1 and z_2

This topic item in addition to the generation of data for 3-D aircraft models using the moment method solution will be pursued pending available time and funds. The experimental verification will be achieved for impedance values z_1 and z_2 at specific frequencies. We now would consider synthesizing these impedances to make the RCS reduction operable over a broad frequency band. From a preliminary examination, the impedance z_1 has all of the properties of a physically realizable structure. We would now attempt the synthesis of that load and examine potential practical techniques for constructing it. The impedance z_2 is not physically realizable. However as we have noted earlier it can be obtained at any single frequency simply by shorting a diode placed across the two conductors of the "folded dipole" at the appropriate position. Thus an adaptive technique could be introduced. First, the system senses the frequency of the radar and then fires the appropriate diode. The goal of this part of the research would be to evaluate the number of diodes to be positioned along the "folded dipole" to obtain the needed RCS reduction over the band when operated in this adaptive mode.

IV. CONCLUSIONS AND RECOMMENDATIONS

The dominant complex natural resonances of radar targets form a minimal set of target descriptors which are excitation invariant. Methods for locating the dominant natural resonances of a target from measured or calculated real-frequency scattering data have not yet been fully optimized. However, the dominant resonances can usually be found provided several target orientations and radar polarizations are tested.

Predictor-correlator processing of a measured transient response from an unknown target provides a target discrimination capability. The method is particularly attractive in that neither the target orientation nor radar polarization need be known. Also, resonances are not extracted from the measured transient response waveform. Experience has shown that present techniques for extracting resonances are not effective with noisy data. Methods for making the prediction-correlation process less susceptable to noise and more easily interpreted have been demonstrated. A very simplified noise analysis has demonstrated basic difficulties and methods for correcting these have been obtained. In short, much has been accomplished but a great deal remains to be done.

There is a basic need to obtain higher frequency scattering data to test how far the concept of nondecayed transients can be pushed. In this regard frequencies selected to exploit substructure resonances such as the vertical or horizontal tail stabilizers on aircraft need to be tested.

Certain of the uncorrected difficulties with Prony's method need to be studied. It is apparent that when pole excitations begin at significantly different times then one exponential approximation starting at the same time will have difficulties. A z-transform version of Prony's method might improve performance and should be tested.

There is evidence that the use of interrogating signals tailored to a particular pole or poles of a given target deserve to be studied. The use of such signals might place certain restrictions on the discrimination range but be much more realizable from a practical viewpoint.

Use of a folded dipole concept for reducing the contribution to RCS caused by the leading conducting edge for a horizontally polarized wave has been considered. This supplements earlier studies for reducing the contribution to the RCS for the trailing edge (for a vertically polarized wave). The technique has been demonstrated to be viable over more than a 10:1 frequency band provided the impedance can be synthesized. It appears that one of these is physically realizable and the other can be achieved by means of an adaptive process. Steps have been suggested in the test that could lead to a practical implementation of these concepts both for the loaded slot for vertically polarized RCS reduction and the loaded folded dipole for horizontally polarized RCS reduction.

APPENDIX - NOISE ANALYSIS

Most of the testing of predictor-correlator processing for target discrimination has used the ramp response waveform as the transient signal received from the unknown target. In References [3,4] however, it was demonstrated that other transient response waveforms could be used. This corresponds to arbitrarily deleting scattering amplitudes and/or phases at certain harmonics. This can be done because the Corrington difference equation holds for any transient response. A major unanswered question at this time is precisely how many and which harmonic scattering data are needed to provide a reasonable discrimination capability. Studies to answer this question are in progresss. This is essentially equivalent to asking which transient scattering signal is best suited for predictor-correlator discrimination. In this regard it will be seen that the ramp weighting (n^{-2}) is not ideal when noise is present. Other weightings such as $n^{-3/2}$, $n^{-7/4}$ etc. are clearly possible. In this appendix ramp waveforms are used exclusively because most of our previous noise-free results were under that condition.

In this initial study it is assumed that the multiple frequency radar supplying the scattering data from the unknown target uses the same transmitter power at each frequency. Because, in the spectral range of interest, the scattered power from the target generally increases with frequency and a ramp weighting is used the signal to noise power at the first two or three harmonics becomes very critical. Therefore the effects of noise shown here should be viewed as a worst possible case. Obviously, with the above knowledge, the system designer would arrange to transmit higher power at the lower harmonics. Provided the noise is not target generated, this would alleviate many of the problems. Studies of these more practical problems are presently in progress. The results obtained in this study are nevertheless of interest, but must be examined within the framework of the above discussion.

When noise is included in the ramp responses of radar targets, the waveform becomes

$$\underset{\sim}{F}_R(t) = F_R(t) + \underset{\sim}{X}(t) \qquad \text{(A1)}$$

where $\underset{\sim}{F}_R(t)$ is the noise-corrupted ramp response, $F_R(t)$ the noise-free ramp response and $\underset{\sim}{X}(t)$ the random noise. A complete analysis of the noise sources will not be attempted here. Only additive noise of a zero-mean stationary normal process will be considered.

Because the postulated radar system synthesizes the ramp response of radar targets from measurements at 10 discrete frequencies, the overall random noise is assumed to be a zero-mean, stationary, normal process having an impulse power spectrum at the 10 discrete frequencies,

$$S_{\tilde{x}}(\omega) = \sum_{n=1}^{10} \frac{90\sigma^2}{\pi^3 n^4} \left[\delta\left(\omega - \frac{2\pi n}{T}\right) + \delta\left(\omega + \frac{2\pi n}{T}\right)\right], \quad -\infty<\omega<\infty \qquad (A2)$$

where the constants are selected such that σ is the standard deviation of the random noise as will be shown later. In Equation (A2), the factor $1/n^4$ is due to the ramp weighting. Because the radar system has a certain bandwidth centered at each of the 10 harmonics, one would like to replace the impulse functions in Equation (A2) by square pulse functions. However this will only complicate the analysis and should not bring out new significant results. Therefore the representation of Equation (A2) seems adequate in this study. The autocorrelation function of the noise is defined as the inverse Fourier transform of $S_{\tilde{x}}(\omega)$,

$$R_{\tilde{x}}(\tau) = \frac{1}{2\pi} \int_{-\infty}^{\infty} S_{\tilde{x}}(\omega)\, e^{i\omega\tau} d\omega = \sum_{n=1}^{10} \frac{90\sigma^2}{\pi^4 n^4} \cos\left(\frac{2\pi n}{T}\tau\right). \qquad (A3)$$

By using the identity [8]

$$\sum_{n=1}^{\infty} \frac{\cos nx}{n^4} = \frac{\pi^4}{90} - \frac{\pi^2 x^2}{12} + \frac{\pi|x|^3}{12} - \frac{x^4}{48} \quad 0\le|x|\le 2\pi, \qquad (A4)$$

Equation (A3) can be simplified with negligible error as

$$R_{\tilde{x}}(\tau) = \sigma^2\left[1 - 30\left(\frac{\tau}{T}\right)^2\left(1 - \frac{|\tau|}{T}\right)^2\right], \quad 0\le|\tau|\le T. \qquad (A5)$$

It follows that the total noise power is

$$R_{\tilde{x}}(0) = \frac{1}{2\pi} \int_{-\infty}^{\infty} S_{\tilde{x}}(\omega)\, d\omega = \sigma^2. \qquad (A6)$$

It is well-known that the total power of a zero-mean, stationary normal process is equal to the variance of the process. Thus σ is the standard deviation of the random noise as was noted earlier.

It has been noted previously that when the fundamental period of the interrogating waveform is sufficiently long, the synthesized ramp waveform will assume a constant value over a portion of the period. To simplify the notation, this constant term will be dropped in the following discussion. The total signal-to-noise power ratio of the ramp response waveform is

$$S_R/N_R = \frac{T^2}{8\pi^4\sigma^2} \sum_{n=1}^{10} \frac{1}{n^4} \left|G\left(\frac{i2\pi n}{T}\right)\right|^2 . \qquad (A7)$$

If Prony's method is applied to the noise-corrupted ramp responses of radar targets, the quantities all become random variables. Theoretically the probability density functions of these quantities can be found and their means and variances calculated. However, to actually carry out the calculations constitutes a very tedious if not impossible task. For example, if five poles are to be extracted, calculation of the means involving integration over at least 10 variables are encountered. Thus it is unwise to proceed in this direction. Suffice to say that because the autocorrelation function $R_{\tilde{x}}(\tau)$ does not vanish for $\tau \neq 0$, sampled values of the ramp response are correlated and therefore the expected values of the poles and the residues are different from the corresponding noise-free values. The amount of change will depend on the signal to noise power ratio and on the location of the resonance in the complex plane. From Equation (A2) it is seen that most of the noise power is concentrated at the first harmonic in contrast to the signal power which is distributed nearly evenly over the 10 harmonics. Therefore if the period T is chosen such that the frequency of the first harmonic is much lower than that of the first resonance of the target, one can anticipate that the noise will have only a small effect on the extracted dominant natural resonances.

In the presence of noise, detection and discrimination capabilities of any scheme will be degraded. The predictor-correlator processing is no exception. The value of ρ' may be substantially lower than unity even if the measured ramp response waveform is that of the target being sought.

To simplify the analysis, assume that F_{R_c}, the calculated waveform, is noise-free and $F_{\tilde{R}_m} = F_{R_m} + \underset{\sim}{x}$, where quantities with the notation $\sim$ are random variables. The assumption of F_{R_c} being noise-free is justified as follows. By using the poles of radar targets (which include a dc pole) one first uses Prony's method to calculate the residues from the measured ramp response through the least squares method. Because the noise power in the measured ramp response concentrates at the first harmonic, the calculated residues will have only small errors except the constant term. However because the constant term can be found from Rayleigh theory and an integration of the synthesized response, the error in the constant term can then be removed. Therefore the calculated ramp response F_{R_c} essentially will contain no noise in a sense that the noise contained in F_{R_c} is much less than that in F_{R_m}.

By retaining low order terms of x one obtained for the normalized error

$$\underset{\sim}{\rho}' = \rho'\left(1 - \frac{\Sigma \underset{\sim}{x}^2}{\Sigma F_{R_m}^2}\right) + 2\,\frac{\Sigma(F_{R_c} - \zeta' F_{R_m})\underset{\sim}{x}}{\Sigma F_{R_m}^2}\left(1 - 2\,\frac{\Sigma F_{R_m}\underset{\sim}{x}}{\Sigma F_{R_m}^2}\right). \qquad \text{(A8)}$$

If the calculated ramp response F_{R_c} is obtained using the natural resonances of the target, $F_{R_c} \approx F_{R_m}$ and the noise-free value of ζ' is very close to 1. Then

$$\rho' = \rho'\left(1 - \frac{\Sigma \underset{\sim}{x}^2}{\Sigma F_{R_m}^2}\right). \qquad \text{(A9)}$$

The expected value of Equation (A9) is

$$E(\underset{\sim}{\zeta}') = \zeta'(1 - N/S), \qquad \text{(A10)}$$

where the noise-to-signal power ratio N/S is different from N_R/S_R of Equation (A7) for the reason to be given later.

The standard deviation of ρ' is

$$\sigma_\rho = a\,\rho'\,N/S \qquad \text{(A11)}$$

where the value of a depends on the autocorrelation function but is approximately equal to unity. Even if F_{R_c} is obtained using natural resonances different from those of the target, the second term in Equation (A8) is small because of cancellation of positive and negative values. Therefore Equation (A9) is generally true independent of the natural resonances.

Equation (A10) shows that the capability of discriminating radar targets using predictor-correlator processing is degraded by a factor of (1 - N/S). The threshold value of $\underset{\sim}{\zeta}'$ to accept the desired target and reject others must be lowered according to the noise-to-signal power ratio. This result would have to be considered a low-noise model.

One can define another noise-to-signal power ratio of the 10 harmonics (without $1/n^4$ weighting)

$$N_o/S_o = \left(\frac{900\sigma^2}{\pi^4}\right)/\left]\,\frac{T^2}{8\pi^4}\sum_{n=1}^{10}\left|G\left(\frac{i2\pi n}{T}\right)\right|2\right]. \qquad \text{(A12)}$$

which is much less than N_R/S_R. Even for small values of N_O/S_O, the noise-to-signal power ratios in the lowest harmonic may be larger than 1. Thus the predictor-correlator processing will discriminate radar targets only if N_O/S_O is very small. This severe condition can be relaxed in the following way. Because the noise-to-signal power ratios in the higher harmonics are lower than those in the lower harmonics, (in the Rayleigh region) then by replacing the measured scattering data of the lower harmonics with values obtained by extrapolating the scattering data of the higher harmonics, the ratio N/S of Equation (A-10) becomes less than N_R/S_R and the predictor-correlator processing can tolerate more noise.

One method of studying the noise effect is to simulate the problem using computer generated random numbers (Monte Carlo method). Reference on computer generated random numbers can be found in Reference [9]. The random numbers generated via a computer using arithmetical methods are uncorrelated. Therefore the random noise process of which the autocorrelation function is given by Equation (A5) can not be generated directly. Digital filters must be used. However, design of digital filters often is a problem. To circumvent this difficulty one takes the following different approach.

If the autocorrelation function of a stationary random process is periodic with period T, i.e.,

$$\underset{\sim}{R}x(\tau) = \sum_{n=-\infty}^{\infty} {}_n e^{i\frac{2\pi n}{T}\tau}, \tag{A13}$$

where

$$\alpha_n = \frac{1}{T}\int_0^T \underset{\sim}{R}x(\tau)\, e^{-i\frac{2\pi n}{T}\tau}\, d\tau, \tag{A14}$$

then the random process can be expanded into a Fourier series [10],

$$\underset{\sim}{x}(t) = \sum_{n=-\infty}^{\infty} \underset{\sim}{a}_n e^{i\frac{2\pi n}{T}t}, \tag{A15}$$

where the coefficients $\underset{\sim}{a}_n$, given by

$$\underset{\sim}{a}_n = \frac{1}{T}\int_0^T \underset{\sim}{x}(t)\, e^{-i\frac{2\pi n}{T}}\, dt, \tag{A16}$$

are uncorrelated and orthogonal random variables. It can be shown that

$$E(\underset{\sim}{a}_n) = E\{\underset{\sim}{x}(t)\}\delta_{no}, \tag{A17}$$

$$E(\underset{\sim}{a}_k \underset{\sim}{a}_n^*) = \alpha_n \delta_{nk}, \tag{A18}$$

where δ_{ij} is the Kronecker delta. These formulas can be applied to the random noise process with autocorrelation function given by Equation (A3). One then finds that

$$\alpha_n = \frac{45\sigma^2}{\pi^4 n^4}, \quad n = -10, -9, \cdots, -1, 1, \cdots, 9, 10, \quad = 0 \text{ otherwise} \tag{A19}$$

Introducing new random variables

$$\underset{\sim}{b}_n = \underset{\sim}{a}_n + \underset{\sim}{a}_n^*, \tag{A20}$$

$$\underset{\sim}{c}_n = i(\underset{\sim}{a}_n - \underset{\sim}{a}_n^*). \tag{A21}$$

Because the random process $\underset{\sim}{x}(t)$ is zero-mean and normal, so are the uncorrelated random variables $\underset{\sim}{b}_n$ and $\underset{\sim}{c}_n$. The standard deviations of $\underset{\sim}{b}_n$ and $\underset{\sim}{c}_n$ are given by

$$\sigma b_n = \sigma_{c_n} = \sigma_n = \sqrt{2\alpha_n}. \tag{A22}$$

The random process

$$\underset{\sim}{x}(t) = \sum_{n=1}^{10} \underset{\sim}{b}_n \cos\left(\frac{2\pi n}{T} t\right) + \underset{\sim}{c}_n \sin\left(\frac{2\pi n}{T} t\right) \tag{A23}$$

is to be used in Equation (A1) which can be rewritten as

$$F_R(t) = \sum_{n=1}^{10} \{[- \frac{T}{2\pi^2 n^2} |G(\frac{i2\pi n}{T})| \cos \phi_n + \underset{\sim}{b}_n] \cos(\frac{2\pi nt}{T})$$

$$+[\frac{T}{2\pi^2 n^2} |G(\frac{i2\pi n}{T})| \sin\phi_n + \underset{\sim}{c}_n] \sin(\frac{2\pi n}{T} t)\} . \quad (A24)$$

Because b_n and c_n are uncorrelated, Equation (A24) can be simulated with computer generated random numbers directly. The statistical properties of Equation (A24) can then be found. Initial tests on the F-4, F-104 and MIG-19 aircraft using computer generated noise were reported in the quarterly letter dated 12 November 1975. The more pertinent tests with the weighting changed as well as the use of the predictor equation are given in the text of this report. The same process was used to generate the noise data.

REFERENCES

[1] Hill, D. A., "Electromagnetic Scattering Concepts Applied to the Detection of Targets Near the Ground," Report 2971-1, September 1970, The Ohio State University ElectroScience Laboratory, Department of Electrical Engineering; prepared under Contract F19628-70-C-0125 for Air Force Systems Command, Laurence G. Hanscom Field, Bedford, Massachusetts. (AFCRL-70-0250) (AD 875889)

[2] Moffatt, D. L., "Time Domain Electromagnetic Scattering from Highly Conducting Objects," Report 2971-2, May, 1971, The Ohio State University ElectroScience Laboratory, Department of Electrical Engineering; prepared under Contract F19628-70-C-0125 for Air Force Systems Command, Laurence G. Hanscom Field, Bedford, Massachusetts. (AFCRL-71-0319) (AD 885883)

[3] Mains, R.K. and Moffatt, D.L.,"Complex Natural Resonances of an Object in Detection and Discrimination," Report 3424-1, June 1974, The Ohio State University ElectroScience Laboratory, Department of Electrical Engineering; prepared under Contract F19628-72-C-0203 for Dept. of the Air Force, Hanscom Air Force Base, Massachusetts. (AFCRL-TR-74-0282)

[4] Moffatt, D. L. and Mains, R. K., "Detection and Discrimination of Radar Targets," IEEE Trans. on Antennas and Propagation, Vol. AP-23, No. 3, May 1975.

[5] Lin, Y. T. and Richmond, J. H., "EM Modelling of Aircraft at Low Frequencies," IEEE Trans. on Antennas and Propagation, AP-23, No. 1, pp. 53-56, January, 1975.

[6] Chuang, C. W. and Moffatt, C. W., Report 3424-3, April 1975, The Ohio State University ElectroScience Laboratory, Department of Electrical Engineering; prepared under Contract F19682-72-C-0203 for Dept. of the Air Force, Hanscom Air Force Base, Massachusetts. (AFCRL-TR-75-0203)

[7] Chuang, C. W. and Moffatt, D. L., "Natural Resonances via Prony's Method and Target Discrimination," IEEE Trans. on Aerospace and Electronic Systems, Vol. 12, No. 5, September, 1976.

[8] Gradshteyn, I. S. and Ryzhik, I. M., Table of Integrals Series and Products, p. 39, Academic Press, 1965.

[9] Hull, T. E. and Dobell, A. R., "Random Number Generators," SIAM Rev., Vol. 4, p. 230, July 1962.

[10] Papoulis, A., Probability, Random Variables, and Stochastic Process, McGraw-Hill, New York, 1965.

References [11] - [14] were prepared under Contract F19628-72-C-0203 by The Ohio State University ElectroScience Laboratory, Department of Electrical Engineering, for Air Force Systems Command, Hanscom Air Force Base, Massachusetts.

[11] Lee, S. C., "Control of Electromagnetic Scattering by Antenna Impedance Loading," Report 3424-2, July 1974. (AFCRL-TR-74-0426)

[12] Aas, J., "Control of Electromagnetic Scattering from Wing Profiles by Impedance Loading," Report 3424-4, August 1975. (AFCRL-TR-75-0463)

[13] Chuang, C. W., "Reduction of Backscattering by Impedance Loading," Report 3424-6, October 1976.

[14] Moffatt, D. L., Rudduck, R. C., Chuang, C. W., Aas, J. A., "Continuation of the Investigation of Multi-Frequency Radar reflectivity and Radar Target Identification," Report 3434-5, July 1975. (AFCRL-TR-75-0417)

MISSION
of
Rome Air Development Center

RADC plans and conducts research, exploratory and advanced development programs in command, control, and communications (C^3) activities, and in the C^3 areas of information sciences and intelligence. The principal technical mission areas are communications, electromagnetic guidance and control, surveillance of ground and aerospace objects, intelligence data collection and handling, information system technology, ionospheric propagation, solid state sciences, microwave physics and electronic reliability, maintainability and compatibility.

☆ U.S. GOVERNMENT PRINTING OFFICE: 1977 700-002/91